iScience

CellPress

Article

Sex-Based *Mhrt* Methylation Chromatinizes MeCP2 in the Heart

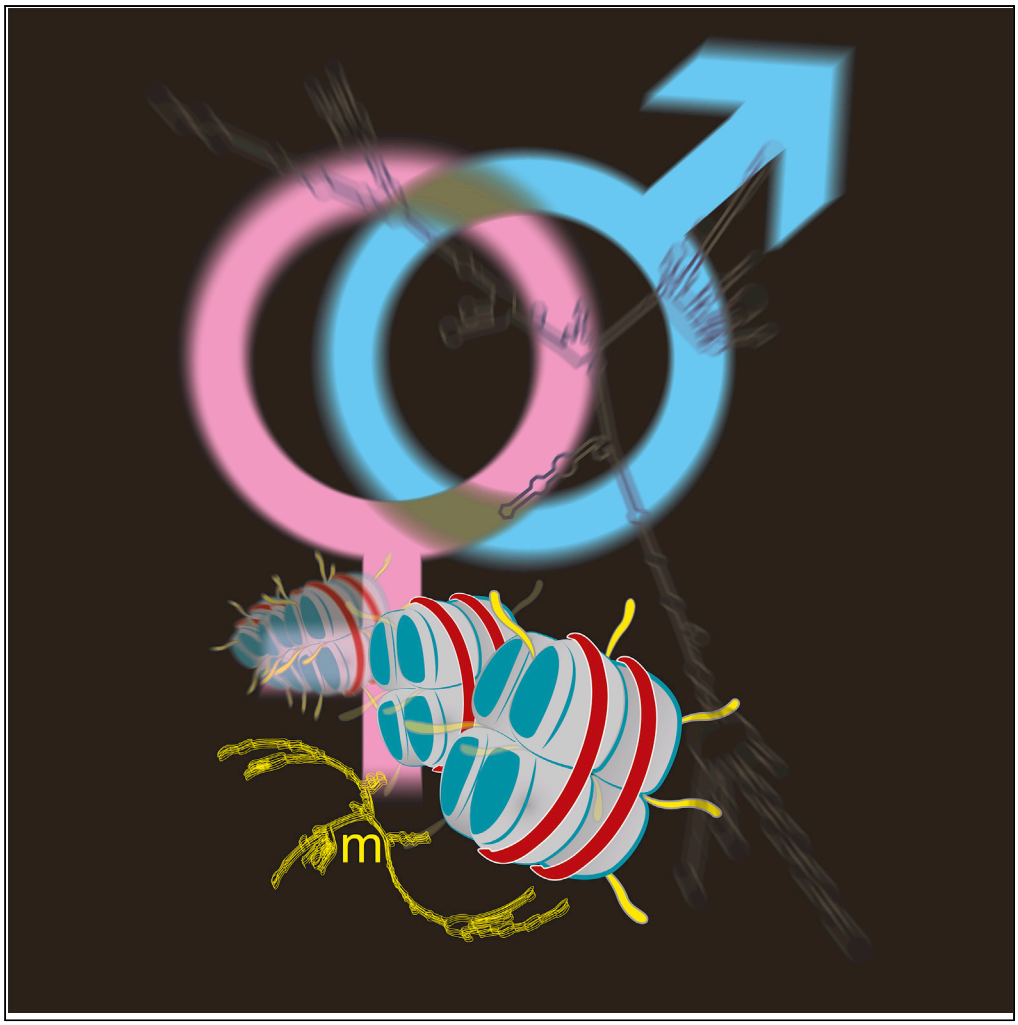

Harikrishnan K.N., Jun Okabe, Prabhu Mathiyalagan, ..., Scott S. Maxwell, Xiao-Jun Du, Assam El-Osta

sam.el-osta@monash.edu

HIGHLIGHTS

Mechanisms underlying sex-based gene expression are poorly understood

Expression of *primary miR-208b* is independent of DNA methylation in the heart

Sex-specific methylation of the long non-coding RNA *Mhrt* distinguishes MeCP2

Procedures assessing soluble chromatin emphasize RNA-dependent affinities

K.N. et al., iScience *17*, 288–301
July 26, 2019
https://doi.org/10.1016/j.isci.2019.06.031

iScience

CellPress

Article

Sex-Based *Mhrt* Methylation Chromatinizes MeCP2 in the Heart

Harikrishnan K.N.,[1,2,3,7] Jun Okabe,[1,2,7] Prabhu Mathiyalagan,[2,6,7] Abdul Waheed Khan,[1,2,3] Sameer A. Jadaan,[1,2,3] Gulcan Sarila,[1,2] Mark Ziemann,[1,2] Ishant Khurana,[1,2] Scott S. Maxwell,[1,2] Xiao-Jun Du,[2] and Assam El-Osta[1,2,3,4,5,8,*]

SUMMARY

In the heart, *primary microRNA-208b* (*pri-miR-208b*) and *Myheart* (*Mhrt*) are long non-coding RNAs (lncRNAs) encoded by the cardiac myosin heavy chain genes. Although preclinical studies have shown that lncRNAs regulate gene expression and are protective for pathological hypertrophy, the mechanism underlying sex-based differences remains poorly understood. In this study, we examined DNA- and RNA-methylation-dependent regulation of *pri-miR-208b* and *Mhrt*. Expression of *pri-miR-208b* is elevated in the left ventricle of the female heart. Despite indistinguishable DNA methylation between sexes, the interaction of MeCP2 on chromatin is subject to RNase digestion, highlighting that affinity of the methyl-CG reader is broader than previously thought. A specialized procedure to isolate RNA from soluble cardiac chromatin emphasizes sex-based affinity of an MeCP2 co-repressor complex with Rest and Hdac2. Sex-specific *Mhrt* methylation chromatinizes MeCP2 at the *pri-miR-208b* promoter and extends the functional relevance of default transcriptional suppression in the heart.

INTRODUCTION

Long non-coding RNAs (lncRNAs) have emerged as important regulators of heart development and disease (Mathiyalagan et al., 2014a; Schonrock et al., 2012). Several lncRNAs such as *Braveheart* (Klattenhoff et al., 2013), *Fendrr* (Grote et al., 2013), *Upperhand* (Anderson et al., 2016), and *Carmen* (Ounzain et al., 2015) are differentially activated at the fetal and adult stages of cardiac development. Although the precise roles of these lncRNAs still remain poorly understood, recent evidence suggests that lncRNAs not only control mRNA expression during the critical transition stages from fetal to adult heart but also function with mRNA stability, decay, and as regulatory sponges (Wang et al., 2014). Not entirely unexpected, in the fetal heart, lncRNAs associate more with genes implicated in processes that involve development and programming, whereas in the adult heart lncRNAs associate more with genes involved in disease. For example, in the adult heart the expression of lncRNAs *Chast* (Viereck et al., 2016), *Chaer* (Wang et al., 2016), and *Wisper* (Micheletti et al., 2017) are linked with cardiac hypertrophy and fibrosis. The sarcomeric myosin heavy chain (MHC) isogenes, originally designated α and β (recently renamed *Myh6* and *Myh7*) are predominantly expressed in the heart (Mahdavi et al., 1982, 1984). During fetal life *Myh7* is principally expressed, whereas *Myh6* and *Myh7* are simultaneously expressed shortly after birth, with *Myh6* dominantly expressed in adulthood (Chizzonite and Zak, 1984; Lompre et al., 1981, 1984). During myocardial hypertrophy *Myh7* is selectively expressed under hemodynamic and pressure overload (Izumo et al., 1987; Litten et al., 1982; Lompre et al., 1979).

Previously known as antisense *β-MHC* (Haddad et al., 2003), *Myosin heavy-chain-associated RNA transcript* (*Myheart, or Mhrt*) is a myocardium-specific lncRNA regulated by antisense transcription of a specific intergenic promoter that originates from the antisense strand of *Myh7* that serves as a switch for *Myh6/7* gene expression (Han et al., 2014). Recent studies have shown that *Mhrt* expression is cardioprotective and behaves as a decoy lncRNA involved in a negative feedback circuit with chromatin remodeling. Interestingly, cardiac hypertrophy induced by pressure overload in a mouse model progressively reduced *Mhrt* expression. Experiments have shown that restoring *Mhrt* to prestress levels can attenuate cardiac damage and rescue the heart from pathological hypertrophy (Han et al., 2014). It is hypothesized that under cardiac stress *Mhrt* restores the *Myh6/7* gene shift by virtue of its interaction with the remodeling enzyme, Brg1, an ATP-dependent DNA helicase and a subunit of a much larger SWI/SNF complex. We have recently shown that *pri-miR-208b*, an lncRNA that originates from *Myh7*, regulates gene expression during cardiac hypertrophy (Mathiyalagan et al., 2014b). Upon transverse aortic constriction (TAC) in a mouse model of

[1]Epigenetics in Human Health and Disease, Central Clinical School, Faculty of Medicine, Monash University, Melbourne, VIC 3004, Australia

[2]Baker Heart and Diabetes Institute, The Alfred Medical Research and Education Precinct, Melbourne, VIC 3004, Australia

[3]Department of Clinical Pathology, The University of Melbourne, Parkville, VIC 3010, Australia

[4]Hong Kong Institute of Diabetes and Obesity, Prince of Wales Hospital, The Chinese University of Hong Kong, 3/F Lui Che Woo Clinical Sciences Building, 30-32 Ngan Shing Street, Sha Tin, Hong Kong SAR

[5]University College Copenhagen, Faculty of Health, Department of Technology, Biomedical Laboratory Science, Copenhagen, Denmark

[6]Present address: Department of Cardiology, Icahn School of Medicine at Mount Sinai, New York, NY 10029, USA

[7]These authors contributed equally

[8]Lead Contact

*Correspondence: sam.el-osta@monash.edu

https://doi.org/10.1016/j.isci.2019.06.031

pathological hypertrophy, the left ventricular tissue shows elevated expression of *pri-miR-208b* that interacts with a Polycomb-group protein, Ezh2, and is part of a Hdac complex that regulates the *Myh6/7* gene shift (Mathiyalagan et al., 2014b). The precise mechanisms regulating sex-based expression of lncRNAs such as *pri-miR-208b* and *Mhrt* remain poorly characterized.

Gender disparity in cardiovascular health and disease is well documented with females generally regarded less vulnerable to pathological cardiac remodeling (Maas and Appelman, 2010). Pathogenic processes such as cardiomyocyte apoptosis and necrosis characteristic of hypertrophy occur predominantly in males (Guerra et al., 1999). Pathological cardiac hypertrophy is characterized by reactivation of fetal gene programming that involves activation of fetal genes and the suppression of genes expressed in adults (Frey and Olson, 2003). This pattern of expression is common to both sexes, whereas molecular remodeling induced by pressure overload hypertrophy occurs predominantly in males (Weinberg et al., 1999; Zhong et al., 2003). Sex differences in the heart are largely determined by steroid hormones; however, several histone modifiers and methyl-binding proteins as well as promoter DNA methylation are closely linked to sex-based gene expression during development and in adult heart (Kurian et al., 2010; Ratnu et al., 2017). The role of lncRNAs in regulating sex-based gene expression by methylation in the heart remain poorly characterized. Because lncRNAs can interact with epigenetic modifiers, our aim was to determine the mechanism of lncRNA methylation in regulating sex-based gene expression in the heart.

MeCP2 is a reader of DNA methylation, a component of a co-repressor complex (Harikrishnan et al., 2005) and recently shown to regulate gene expression in chronic heart failure (Mayer et al., 2015). In addition to its high affinity for methylated cytosine sites on DNA, MeCP2 is recognized for its ability to bind RNA and regulate alternative splicing events by interacting with YB-1 (Young et al., 2005; Long et al., 2011; Jeffery and Nakielny, 2004). Although MeCP2 was initially characterized as a reader with high affinity for methylated cytosine in DNA (Bird and Wolffe, 1999), more recent studies have shown that MeCP2 can interact with other RNAs (Maxwell et al., 2013; Khan et al., 2017b, 2017c). For example, MeCP2 has been shown to interact with mRNAs (Long et al., 2011); non-coding RNAs (ncRNAs) such as *let-7i*, *miR-375*, and *miR-126* (Khan et al., 2017c); as well as *Rncr3* and *Malat1* (Maxwell et al., 2013). Although these studies suggest that MeCP2 interacts with RNA to suppress gene expression, the mechanism mediated by lncRNA in the myocardium remains poorly understood.

One mechanism recently identified in the epigenetic control of lncRNAs is the deposition of 5-methylcytosine (5mC) (Squires et al., 2012; Amort et al., 2013). This epigenetic determinant occurs on coding RNA and ncRNA, and several lncRNAs such as *Xist*, *Hotair*, and *Malat1* contain 5mC sites and have been shown to regulate ncRNA function (Amort et al., 2013, 2017). The purpose of this study was to explore the sex-based differences in lncRNA expression in the heart. Recent studies have shown that RNA-dependent MeCP2 binding on genes is independent of DNA methylation (Khan et al., 2017b). Therefore, we hypothesized that sex-based interaction of MeCP2 at the pri-miR-208b promoter is associated with *Mhrt* lncRNA methylation. Close examination of DNA methylation at the *pri-miR-208b* promoter using bisulfite sequencing identified nine sites of cytosine methylation at the CpG island (CGI). We observed no difference in DNA methylation between the sexes but show dramatic changes in the binding of the methylation reader, MeCP2, on the *pri-miR-208b* promoter using chromatin immunoprecipitation (ChIP). We identified that sex-specific expression of *pri-miR-208b* in the female heart is independent of DNA methylation. We provide proof of concept that MeCP2 affinity to chromatin is subject to RNA-methylation-dependent regulation. Sex-specific methylation of *Mhrt* distinguishes MeCP2 chromatinization of the *pri-miR-208b* promoter and gene regulation in the female heart.

RESULTS

Sex Differences in *Primary miR-208b* Expression in the Heart

In the heart, cardiac myosin heavy chain (*Myh*) genes are transcriptionally regulated by distinct promoters that give rise to protein-coding genes and ncRNA production (Figure 1A). Located between *Myh6* and *Myh7* genes (Han et al., 2014; Mathiyalagan et al., 2014b) the promoter serves to regulate the transcription of the antisense lncRNA, *Mhrt*. To investigate gender differences in ncRNA expression we used qRT-PCR. *Myh*-encoded RNAs show sex-based differences in the expression of *pri-miR-208b* and *Myh6* in female left ventricles when compared with males (Figures 1B and 1C). In contrast, we observe no significant differences in the expression of *Myh7*, *Mhrt*, and mature *miR-208b* transcripts (Figures 1D–1F).

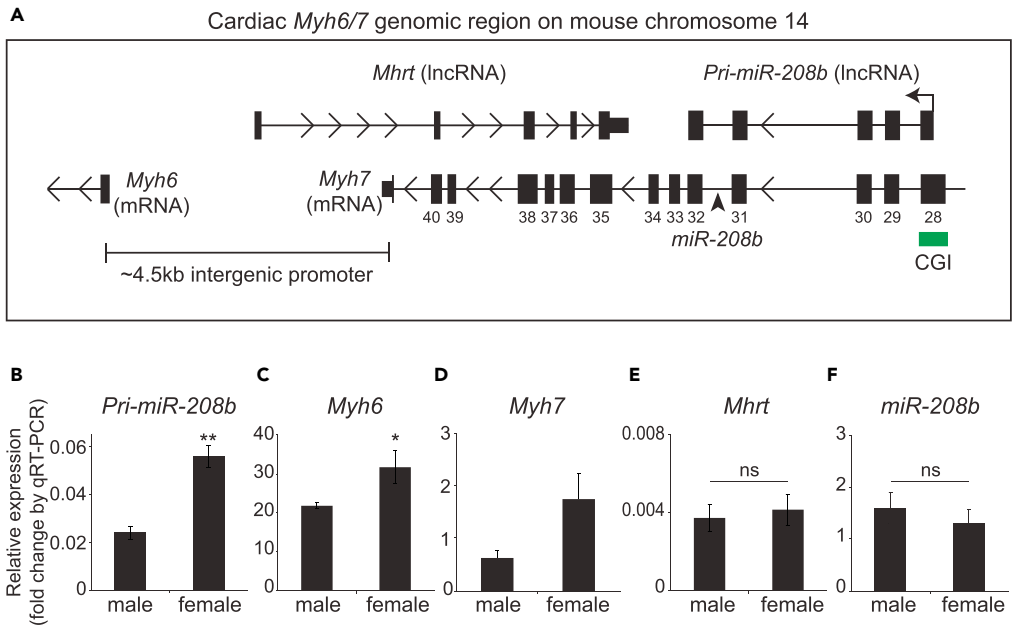

Figure 1. Elevated *Primary miR-208b* (*pri-miR-208b*) Transcript in Female Left Ventricle

(A) Genomic organization of myosin heavy chain coding and non-coding genes on chromosome 14 of mouse. qRT-PCR quantification of (B) *pri-miR-208b*; (C) *Myh6*; (D) *Myh7*, p = 0.065; (E) *Mhrt* (also known as antisense *β-MHC*); and (F) *miR-208b*. Normalized to *Gapdh*. CGI, CpG island; TSS, transcription start site; ns, not significant. *p < 0.05, **p < 0.01. n = 5 mice per group. Data are represented as mean ± SEM.

To understand the regulation of *pri-miR-208b* transcript, we examined its promoter located within exon 28 of mouse *Myh7* gene (Figure 2A) (Monteys et al., 2010; van Rooij et al., 2009). The majority of RNA Pol II promoters are marked by CGI (Lujambio and Esteller, 2007; Carninci et al., 2006; Ozsolak et al., 2008) and served by specific bidirectional promoters (bdPs) (Trinklein et al., 2004). The promoter initiating *pri-miR-208b* transcription has a CGI that is conserved between mouse and human *Myh* orthologs (Figure 2A, CGI shown in green). Bisulfite sequencing identified nine CG sites (located at positions 14, 19, 20, 22, 23, 24, 25, 27, and 28) that are methylated in the promoter but were indistinguishable between male and female heart tissues (Figure 2B). Although these results suggest that *pri-miR-208b* promoter is methylated at specific CG dinucleotides, DNA methylation alone does not explain sex-based differences in *pri-miR-208b* expression.

Sex-Specific Affinity for MeCP2 with *Pri-miR-208b* Chromatin Is RNA Dependent

Methyl-CpG-binding protein-mediated gene suppression involves the recognition of DNA methylation at CG dinucleotides at gene promoters, and recent experimental evidence implicates a regulatory role for MeCP2 in the mouse heart (Mayer et al., 2015). As *pri-miR-208b* promoter is methylated we assessed expression and chromatin interaction of methyl CpG-binding proteins in male and female hearts. qRT-PCR analysis shows no significant differences in the expression of *Mecp2*, *Mbd1*, *Mbd2*, and *Mbd3* transcripts between the sexes (Figure S1). As the *pri-miR-208b* promoter is methylated albeit indistinguishably between sexes, we examined the binding specificities of protein readers of DNA methylation, members of the methyl-CpG-binding domain assessed by ChIP assays. Antibodies that specifically recognize MeCP2, MBD1, MBD2, and MBD3 were used to immunopurify soluble chromatin, followed by nucleic acid purification and quantification by qPCR. This technique specifically detects chromatin-bound MeCP2 fractions, whereas the protocol does not distinguish RNA-dependent interactions (Figure 2C, –RNase A). The specificity of antibody enrichment for *pri-miR-208b* chromatin was also assessed using IgG antibody controls (data not shown). As shown in Figure 2D, soluble chromatin was significantly enriched for MeCP2 on the *pri-miR-208b* promoter when compared with antibodies that recognize the other methyl-CpG-binding proteins. We also observed sex-based differences in chromatinized MeCP2 on the *pri-miR-208b* promoter (Figure 2D, –RNase A). We confirm that the affinity for MeCP2 was specific for the *pri-miR-208b* promoter

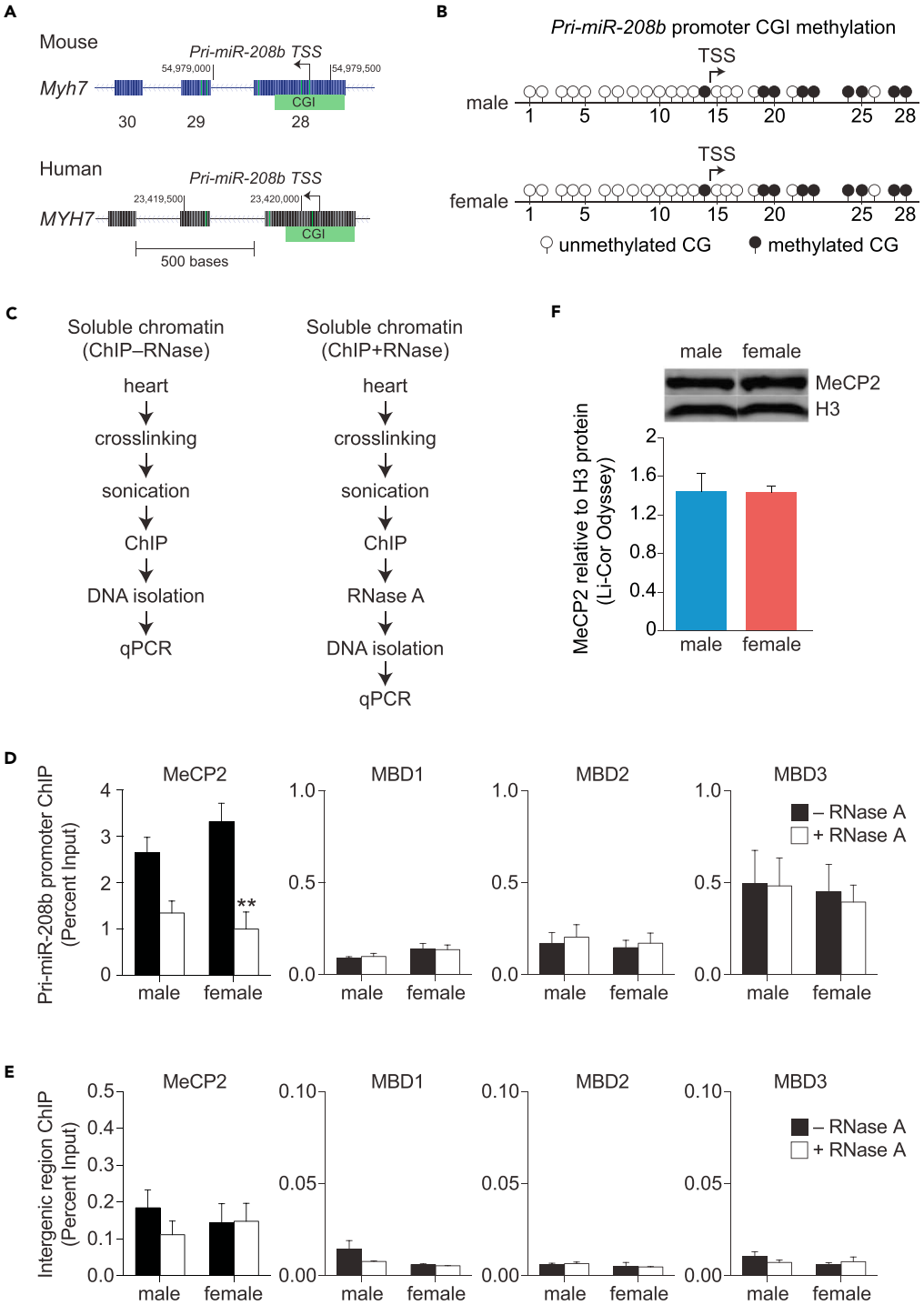

Figure 2. Interaction of the MeCP2 Reader on the *pri-miR-208b* Promoter in Female Left Ventricle Is Independent of DNA Methylation and Involves RNA Interactions

(A) Exon 28 of *Myh7* gene showing *pri-miR-208b* promoter with CpG Island (CGI). CGI sequence within *pri-miR-208b* promoter is conserved between mice and humans.

(B) Bisulfite conversion and DNA methylation show site-specific CG methylation in male and female left ventricle (LV).

(C) Procedure of ChIP coupled with ribonuclease degradation (+RNase A) to assess cardiac RNA-dependent interactions.

(D and E) (D) Specific binding of MeCP2 at *pri-miR-208b* promoter in male and female LV in the presence (+) or absence (–) of RNase A. (E) Intergenic promoter is shown as a control for methyl CpG-binding proteins.

Figure 2. *Continued*

(F) Representative immunoblots of MeCP2 protein expression in male and female LV. Bar graph represents mean values of LI-COR Odyssey quantification of protein blots normalized to histone H3.

**p < 0.01. n ≥ 4 mice per group. Data are represented as mean ± SEM. See also Figure S1.

when compared with the intergenic region (Figure 2E). Because these results were inconsistent with DNA methylation observed at the *pri-miR-208b* promoter (Figure 2B) we proposed that sex-based differences in MeCP2 affinity on soluble chromatin could be RNA dependent.

To test this hypothesis further, we devised a ChIP protocol that involves ribonuclease degradation (Figure 2C, +RNase A) to assess cardiac RNA-dependent MeCP2 affinity with the *pri-miR-208b* promoter (Khan et al., 2017b, 2017c; Maxwell et al., 2013; Mathiyalagan et al., 2014b). To test the feasibility of this approach, soluble MeCP2-associated chromatin fractions were subject to endoribonuclease A (+RNase A) to catalyze the cleavage of chromatin-associated RNA molecules. We observed significant reduction of MeCP2 affinity on the *pri-miR-208b* promoter in RNase-treated cardiac chromatin (Figure 2D, +RNase A). Furthermore, the qPCR signal for MeCP2 by ChIP was reduced for the *pri-miR-208b* promoter in the female heart. To confirm that the loss of MeCP2 binding following RNase exposure was specific for the *pri-miR-208b* promoter, we also assessed the intergenic region that is known to give rise to *Myh6/Myh7* transcript diversity. Irrespective of sex we recovered the intergenic region equally well from chromatin isolates using MeCP2 antibody (Figure 2E). Furthermore, we assessed fractionated MeCP2 protein levels in the heart. Quantitative analysis of MeCP2 using LI-COR Odyssey imaging system show comparable protein expression from male and female heart tissue (Figure 2F), which is consistent with comparable mRNA expression (Figure S1). Taken together, these experimental results derived from soluble chromatin fractions using specific endoribonuclease assays further reinforce the view that *pri-miR-208b* promoter is subject to RNA-dependent MeCP2 binding.

Affinity of Rest and Hdac2 on *Pri-miR-208b* Chromatin Is RNA Dependent

MeCP2 binds methylated DNA on assembled chromatin to recruit the RE1-silencing transcription factor (Rest) and histone deacetylase 2 (Hdac2) to repress gene transcription (Noh et al., 2012; Ooi and Wood, 2007). *In silico* analysis of *pri-miR-208b* promoter shows transcription factor-binding sites for Rest co-repressor protein (Figure S2). We assessed whether Rest and Hdac2 affinities for the *pri-miR-208b* promoter are subject to RNA-mediated interactions using specific ChIP assays. Consistent with previous results in the female heart, we observe reduced binding of Rest on the *pri-miR-208b* promoter by ChIP (–RNase A) and confirm that RNA is a substrate for binding (+RNase A), as shown in Figure 3A. Specificity for the *pri-miR-208b* promoter was shown by near-comparable Rest binding with the intergenic promoter in both sexes. Apart from the requirement for RNA to bind Rest to the *pri-miR-208b* promoter we observe no distinguishable difference at the intergenic promoter (Figure 3A). We also assessed Hdac2-associated chromatin fragments and confirm that affinity for the *pri-miR-208b* promoter is sensitive to nuclease degradation and in part mediated by RNA (Figure 3B, +RNase A). Taken together, these observations strengthen the view that sex-based affinity of the co-repressor complex at *pri-miR-208b* promoter is sensitive to endoribonuclease digestion and thus places specific emphasis on RNA-dependent interactions.

Mhrt Forms Stable RNA:dsDNA Hybrid with *Pri-miR-208b* Promoter

lncRNAs have emerged as a class of gene regulators that serve to alter chromatin structure and gene function (Mercer and Mattick, 2013; Mathiyalagan et al., 2014a). lncRNAs can form stable RNA-DNA hybrids and act as docking sites for transcription factors (Schmitz et al., 2010; Grote et al., 2013; Mathiyalagan et al., 2014b; Place et al., 2008). A recent study has shown that stress-induced interaction of *Mhrt* with the Brg1 complex regulates the *Myh6/7* gene shift in the heart (Han et al., 2014). Therefore, we assessed whether *Mhrt* could bind the *pri-miR-208b* chromatin. *In silico* analysis identified a 37-nucleotide (nt) binding site for *Mhrt* RNA (CG8-9 correspond to positions 141–178: Figure S3) downstream of the *pri-miR-208b* transcription start site (Figure 3C). To assess whether *Mhrt* could form stable hybrid (RNA:dsDNA [double-stranded DNA]) with *pri-miR-208b* promoter, we performed binding assays using *Mhrt* RNA oligomer corresponding to the 37-nt sequence and dsDNA matching the *pri-miR-208b* promoter sequence (Grote et al., 2013; Mathiyalagan et al., 2014b). Because the RNA oligomer (RNAmer) was constructed with biotin label at the 3′ end of *Mhrt* this allowed for immunopurification using streptavidin beads. Incubation of RNA and dsDNA followed by streptavidin capture and qPCR amplification of *pri-miR-208b* promoter shows high affinity for the *Mhrt* oligomer (Figure 3D, –RNase). However, in the presence of RNase H, which specifically

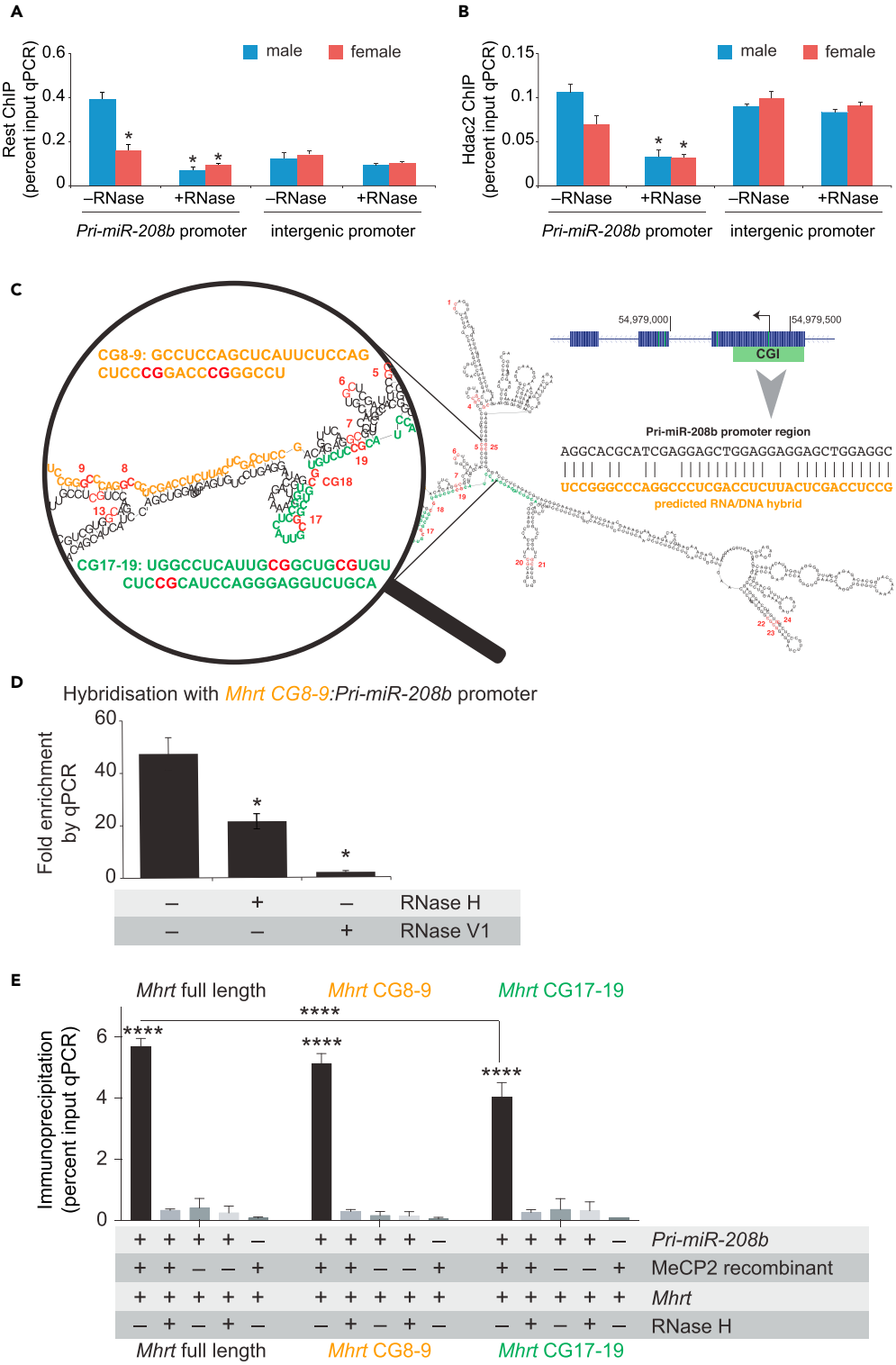

Figure 3. MeCP2 Forms an RNA/dsDNA Hybrid with *Mhrt* and *pri-miR-208b*

(A and B) Chromatin immunoprecipitation of (A) Rest and (B) Hdac2 binding at *pri-miR-208b* promoter in male and female LV in the presence (+) or absence (–) of RNase A.

(C) Enlarged view of the RNA/DNA hybrid region in predicted secondary structure of full-length *Mhrt* (also shown in Figure S3). The predicted *Mhrt* lncRNA (shown in orange)/DNA hybrid sequence at the *pri-miR-208b* promoter (shown in black). Twenty-five CG dinucleotides of *Mhrt* lncRNA are shown in red.

Figure 3. *Continued*

(D) *In vitro* reconstitution assay showing qPCR amplification of *pri-miR-208b* promoter after hybridization with *Mhrt* oligomer in the presence of RNase H or RNase V1.

(E) Amplification of *pri-miR-208b* promoter by qPCR after MeCP2 immunopurification from the *Mhrt* RNA-dsDNA hybrid. *p < 0.05. ****p < 0.0001. Data are represented as mean ± SEM. See also Figures S2–S4.

cleaves RNA in an RNA:dsDNA hybrid (Grote et al., 2013; Mathiyalagan et al., 2014b), the qPCR signal for *pri-miR-208b* was significantly reduced (Figure 3D, +RNase H). To further illustrate the specificity of RNA binding we used RNase V1, which cleaves base-paired RNA nucleotides (Grote et al., 2013; Lee et al., 2010), to confirm that *Mhrt* interacts directly with *pri-miR-208b* promoter (Figure 3D, +RNase V1).

Because MeCP2 binding is sensitive to RNA nuclease degradation we assessed binding to RNA:dsDNA hybrids. To do this, binding assays were performed using recombinant MeCP2 in the presence or absence of RNA (full-length *Mhrt*):dsDNA (*Pri-miR-208b*) hybrids. We made use of selective mixtures of RNA:dsDNA hybrids to test the sensitivity to RNase H nuclease digestion following immunopurification using an antibody that specifically recognizes MeCP2. Isolated DNA was assayed by qPCR detection of the *pri-miR-208b* promoter (Figure S4). Under optimal binding conditions, we observe no qPCR signal for the *pri-miR-208b* promoter using the MeCP2 antibody. Under identical reaction conditions, we found that MeCP2 was significantly enriched on the *pri-miR-208b* promoter in the presence of full-length *Mhrt* RNA (Figure 3E). RNA transcripts fold into secondary structures critical to form RNA-DNA interactions as predicted by the minimal free energy of *Mhrt* transcript (Figure S3). Interestingly, CG18 is the nearest dinucleotide site in the hybrid region (Figure 3C). To assess the hybrid region of *Mhrt* transcript, we performed MeCP2 binding assays using CG8-9 and CG17-19 *Mhrt* RNAmers as well as the full-length *Mhrt* transcript (Figure 3E). CG8-9 and CG17-19 displayed strong affinity for recombinant MeCP2 protein. To test the binding specificity under identical reaction conditions we also assessed the interaction of recombinant Set7 methyltransferase, which does not recognize methylated DNA. We confirm that Set7 does not interact with the RNA:dsDNA hybrid (personal observations). The interaction of MeCP2 with *Mhrt* and *pri-miR-208b* duplex led us to examine whether this affinity was sensitive to RNase H nuclease digestion. Following MeCP2 immunoprecipitation capture the signal for *pri-miR-208b* promoter was barely detectable. These results support the view that MeCP2 affinity for the *pri-miR-208b* promoter is mediated by CG8-9 and CG17-19 interaction for *Mhrt* lncRNA.

Mhrt Methylation Distinguishes Sex-Based Differences in MeCP2 Binding

Because *Mhrt* has been shown to function as decoy lncRNA by interacting with Brg1 in cardiac hypertrophy (Han et al., 2014), we hypothesized that *Mhrt* could interact with MeCP2. To do this, we isolated RNA from soluble chromatin fractions immunopurified using anti-MeCP2 antibody, and tested binding affinities for *Mhrt* using qPCR detection. We observe sex-based differences for MeCP2 affinity on *Mhrt* using a specific RNA-ChIP procedure (Figures 4A and S5). The affinity of MeCP2 for *Mhrt* was significantly reduced in +RNase A-treated chromatin when compared with IgG antibody controls (Figure S5). Although these results imply MeCP2 interacts with *Mhrt*, the affinity for the lncRNA remains poorly characterized.

Recent studies show that post-transcriptional RNA modifications are implicated in transcriptional control (Amort et al., 2013; Squires et al., 2012). We hypothesized that the affinity of the methylation reader MeCP2 is dependent on 5mC deposition on *Mhrt* lncRNA. To do this we examined the possible methylation sites at 25 CG dinucleotides (Figure S6) using bisulfite sequencing of five distinct regions labeled A-E that cover the *Mhrt* lncRNA (Figure 4B). RNA methylation analysis showed sex specific methylation at CG18 position detectable in 25% of total clones tested for this site in female heart tissues (Figure 4C). We observed no RNA methylation for other CG sites of the *Mhrt* transcript in male and female hearts. These results suggest that specific cytosine methylation at position CG18 of *Mhrt* could distinguish sex-specific affinity for MeCP2.

MeCP2 Binds Methylated *Mhrt* lncRNA

To investigate site-specific *Mhrt* methylation and MeCP2 interaction, we designed biotin-tagged synthetic RNAmers that include CG17, CG18, and CG19 sites of the *Mhrt* transcript (Figure 4D). The CG18 site of the *Mhrt* transcript is conserved in humans and mice, suggesting that it could be important for MeCP2 affinity (Figure S6). To specifically examine methylation at CG18 we designed RNAmers that replaced cytosine residues with adenosine (Figure 4D). *Mhrt* oligomer-1 contained three CGs intact (CG17-19), oligomer-2

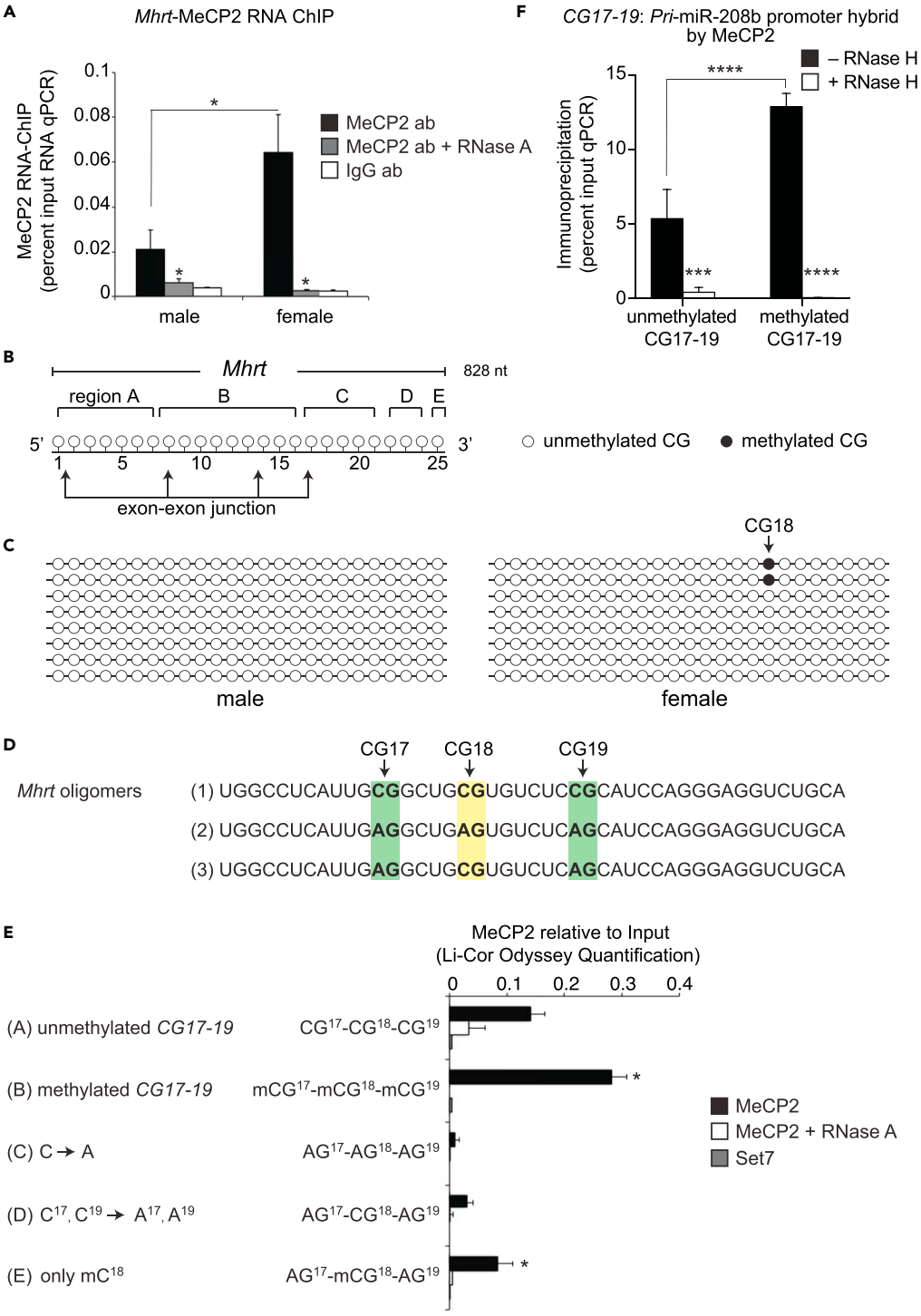

Figure 4. *Mhrt* Is Methylated and Binds to MeCP2 in Female Left Ventricle

(A) RNA-ChIP using anti-MeCP2 antibody showing *Mhrt* interaction with MeCP2-bound chromatin in male and female left ventricle (LV). n = 6 mice per group.

(B) Illustration of 0.828 kb of *Mhrt* lncRNA with 25 CG dinucleotides and regions A-E targeted by bisulfite primers.

(C) Bisulfite-converted *Mhrt* clones showing methylation at CG18 of *Mhrt* lncRNA in female LV. n = 5 mice per group.

(D) Synthetic 45-nt-long *Mhrt* oligomer highlighting CG17-19 and variants with replaced cytosine to adenosine residues.

Figure 4. *Continued*

(E) Quantification of *Mhrt*-MeCP2 binding assay showing enhanced MeCP2 binding after methylation of synthetic *Mhrt* oligomer.

(F) RNA-dsDNA hybrid binding assay showing methylation-dependent affinity of MeCP2 for CG17-19 *Mhrt* RNAmer.

*p < 0.05, ***p < 0.001, ****p < 0.0001. Data are represented as mean ± SEM. See also Figures S5–S8.

contained "C" replaced with "A" at all three sites, and oligomer-3 contained "C" replaced with "A" only at CG17 and CG19, thus leaving CG18 intact. To assess the affinity for methylated CG18, RNAmers were reconstituted with recombinant MeCP2 followed by immunopurification using streptavidin beads. Quantitative protein blotting using LI-COR Odyssey was performed using an antibody that specifically recognizes MeCP2 (Figure S7). To assess MeCP2 affinity for the methylated and unmethylated RNAmers *M.Sss1* methyltransferase (Flynn et al., 1996) was used to specifically methylate CG17-19 sites. We observed binding of recombinant MeCP2 when incubated with unmethylated CG17-19 *Mhrt* RNAmer (Figure 4E, panel A); however, the affinity for MeCP2 was significantly enriched in the presence of methylated CG17-19 *Mhrt* RNAmer (Figure 4E, panel B). Binding for MeCP2 was competed when incubated with oligomer-2, suggesting that the CG18 site is an important substrate for binding (Figure 4E, panel C). In support of this viewpoint, the affinity of MeCP2 was restored when site position CG18 was methylated using oligomer-3 (Figure 4E, panel E) when compared with the unmethylated version (Figure 4E, panel D). Furthermore, we confirm that MeCP2 affinity was RNA dependent using ribonuclease A (Figure 4E, MeCP2+RNase A). To illustrate the specificity of MeCP2 affinity for *Mhrt* we assessed binding of the lysine methyltransferase writer Set7, which neither distinguishes methylated DNA nor binds RNA. We confirm that Set7 does not interact with methylated RNAmers, confirming the affinity of MeCP2 for methylated *Mhrt* at CG18 site (Figure 4E). These results support the view that CG18 methylation could account for MeCP2 affinity to *Mhrt* lncRNA. Based on these results we examined the expression of known RNA methyltransferase transcripts (*Nsun2*, *Nsun4*, *Nsun5*, *Rnmt1*, *Nop2*, *Trdmt1*, *Mrm1*, *Trmt1*) in male and female tissues. There was no significant difference in the expression of RNA methyltransferases (Figure S8).

To assess whether *Mhrt* methylation influences the affinity of MeCP2-dependent formation with *pri-miR-208b* promoter, we performed RNA:dsDNA hybrid assays using methylated/unmethylated CG17-19 *Mhrt* RNAmers (oligomer-1 in Figure 4D). We made use of selective mixtures of RNA:dsDNA hybrids to test the sensitivity to RNase H digestion following immunopurification using an antibody that specifically recognizes MeCP2. Isolated DNA was assayed by qPCR detection of the *pri-miR-208b* promoter (Figure S4). Consistent with the binding affinity of MeCP2 with *Mhrt* in the female heart, MeCP2 was significantly enriched on the *pri-miR-208b* promoter when *Mhrt* is specifically methylated at CG17-19 following capture by RNA immunoprecipitation (Figure 4F –RNase H). The qPCR signal for the *pri-miR-208b* promoter was almost abolished using identical binding conditions and ribonuclease endonuclease H enzyme that catalyzes the cleavage of RNA in an RNA/DNA hybrid (Figure 4F + RNase H). Taken together, these results suggest that the affinity of MeCP2 for the RNA:dsDNA hybrid is likely to depend on *Mhrt* methylation to chromatinize the *pri-miR-208b* promoter to regulate gene transcription.

DISCUSSION

Although sex-based differences in the incidence, prevalence, and severity of cardiovascular disease are well documented the functional mechanisms underlying sex-specific gene expression remains poorly understood. Whether sexual dimorphism is functionally regulated by methylation of DNA and RNA nucleobases remains uncharted in the heart.

It is probable that methylation of *Mhrt* that we describe is responsible for sex-based differences in *pri-miR-208b* expression. The proposed model is mediated by DNA methylation, which we speculate is functioning in a context-dependent manner on the *pri-miR-208b* promoter and distinct from the exclusive RNA methylation observed in *Mhrt* in females. This is because, irrespective of sex, the *pri-miR-208b* promoter is characterized by CGI methylation at nine identical sites. Close inspection of *Mhrt* and *pri-miR-208b* lncRNAs shows several interesting features. First, *Mhrt* is methylated in female heart tissue and the presence of RNA methylation at the CG18 site may indicate regulatory function that is associated with MeCP2 affinity. Second, irrespective of sex the *pri-miR-208b* promoter is methylated at nine identical CG sites and represents default repression. We believe that interactions mediated by DNA and RNA methylation are context specific, meaning MeCP2 assembles on methyl-CG sites and cooperatively serves to suppress gene expression. It should be stressed, however, that we are not suggesting a hierarchy of affinity, rather a

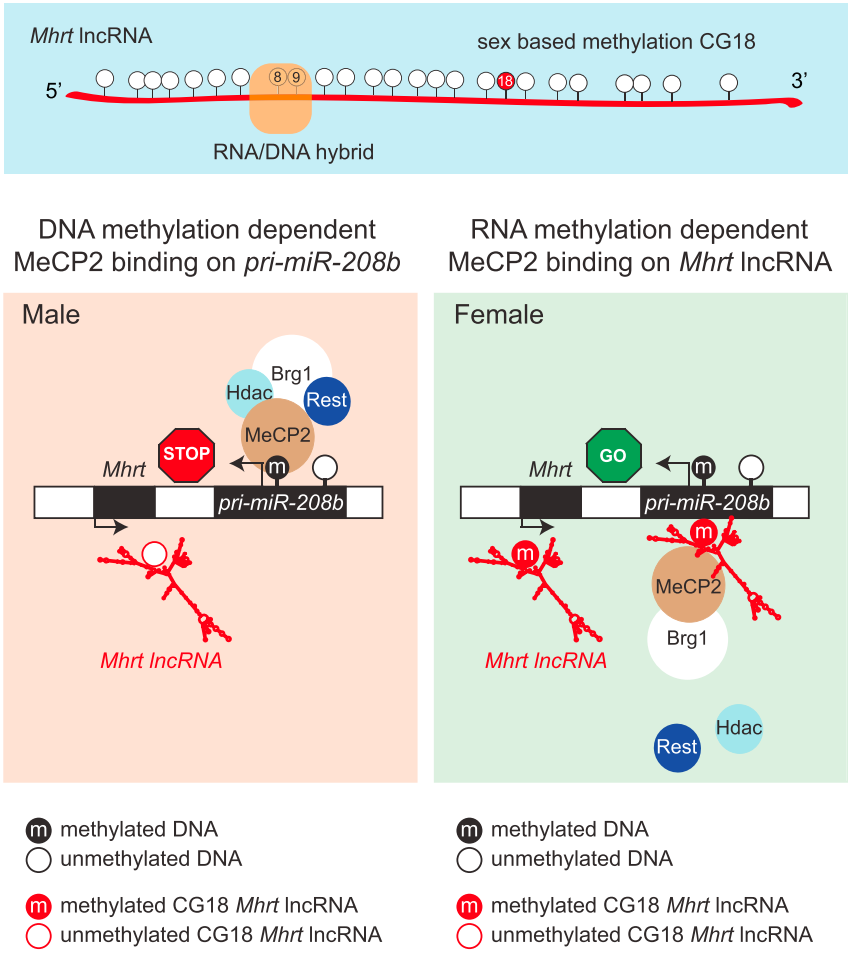

Figure 5. Working Model Based on Current Knowledge

Cooperative DNA and sex-based RNA methylation in the heart. In this study, we identify the *pri-miR-208b* promoter hybrid region and sex-based methylation site (CG18) of *Mhrt* lncRNA. We postulate that the methylation reader MeCP2 and the co-repressor protein complex interact with the *pri-miR-208b* promoter because the *Mhrt* lncRNA is unmethylated at CG18 in the male heart. Methylation at position CG18 of *Mhrt* lncRNA is observed with enriched MeCP2 interaction in the female heart allowing *pri-miR-208b* transcription. *Mhrt* lncRNA is also linked with the SWI/SNF-binding determinant Brg1 (Han et al., 2014).

cooperative association. It has been commonly assumed that the 5mC determinant on DNA is the predominant target of methylation readers (Harikrishnan et al., 2005). We propose that the 5mC-dependent reader, MeCP2 co-repressor complex, targets the *pri-miR-208b* promoter to suppress expression in the male heart. Although methylation-mediated transcriptional silencing by MeCP2 is well documented (Nan et al., 1997), recent studies in animal and human cells have shown broader binding preferences that include mRNA (Long et al., 2011), double-stranded RNA (Jeffery and Nakielny, 2004), short-(Khan et al., 2017b) and long-ncRNAs (Maxwell et al., 2013), as well as RNA-dependent spliceosome and miRNA-processing determinants (Young et al., 2005; Cheng et al., 2014). Thus, although the conventional view of MeCP2-mediated suppression parallels our observations of DNA methylation in the heart, we hypothesize that RNA methylation could signal MeCP2. So how does *Mhrt* alleviate *pri-miR-208b* suppression in the female heart? As a resolution to this problem, rather than querying MeCP2 interaction solely with methylated DNA, we also assessed the affinity of MeCP2 with *Mhrt* lncRNA as a prime candidate for transcriptional control. This mode of regulation requires specialization, and *Mhrt* is a prime substrate for MeCP2, which is exclusively methylated in females (Figure 5). This context-dependent default repression (Tsang et al., 2007) ensures that *pri-miR-208b* is continually turned off when the promoter is methylated in the (male) heart but turned on when *Mhrt* lncRNA is methylated at CG18 (in the female heart). This is an argument supported by emerging experimental evidence showing RNA methylation as a functional regulatory signal in gene

control (Amort et al., 2013, 2017; Squires et al., 2012) and in keeping with observations we describe for MeCP2-mediated binding of the lncRNA, *Mhrt*. At the molecular level, this mode of regulation could account for the transcriptional robustness in *pri-miR-208b* expression in the female heart as well as the capacity for sex-based expression, notwithstanding identical CGI methylation at the *pri-miR-208b* promoter.

RNA methylation of cardiac *Mhrt* extends the functional importance of MeCP2-mediated gene silencing. Nowhere is this more evident than in the signaling molecules that assemble on, and serve to, chromatinize the regulatory cross talk between DNA and RNA (Khan et al., 2017b, 2017c). There are several advantages to MeCP2 coordinating context-dependent regulation. First, 5mC is an effective target for MeCP2. Binding experiments have shown remarkable specificity for the nuclear protein, revealing that a single symmetrical methylated CG site is sufficient for MeCP2 binding (Nan et al., 1996; Meehan et al., 1992) and that hemi-methylated DNA is a poor substrate (Lewis et al., 1992). Second, on methylated CG sites MeCP2 forms a stable complex with HDAC activity to repress transcription. Of note, methylated DNA assembled into chromatin binds MeCP2 and resides in a complex that co-purifies with members of the DNA helicase/ATPase family such as ATRX (Nan et al., 2007), Brahma (Harikrishnan et al., 2005), Brg1 (Hwang et al., 2009), and Mi-2 (Wade et al., 1998). The ability of MeCP2 to bind to methylated nucleobases to form cell- and tissue-specific regulatory complexes serves to precisely control gene regulation in the heart. In the above examples, CG methylation is the predominant determinant. In other cases, MeCP2 can impart specificity by virtue of interactions with the DNA methylation writing enzyme, DNMT1, to target candidate sequence elements to repress transcription (Robertson et al., 2000). Once again, the effectiveness of MeCP2 to achieve gene control relies on its capacity to interpret and tightly bind methylated CG sites. Clearly, methylation-mediated regulation is complicated; however, the diversity in the mechanism of action by the methyl moiety interpreted by MeCP2 represents an attractive solution to connect what appear to be distinct and even seemingly unconnected signaling pathways (Simpson, 2015). This is strikingly reminiscent of the norepinephrine pathway leading to MeCP2 repression upon activation of α1- and β1-adrenoceptors in cardiomyocytes (Mayer et al., 2015). In a mouse model of pathological hypertrophy using TAC the specific CG methylation sites of target genes under direct regulation by MeCP2 remain unaltered. Cardiomyocytes derived from Sham animals show methylation-mediated suppression of *Ppargc1a* by MeCP2, whereas in TAC animals the induction of *miR-212/132* removes MeCP2 from the same methyl-CG sites. Although that study (Mayer et al., 2015) did not examine sexual dimorphism in sympathetic cardioprotective pathways, it shows that dynamic signaling gradients can shape MeCP2 regulation and default repression mechanisms in hypertrophic hearts.

Important clinically, pathological signaling can integrate regulatory pathways to connect methylation of assembled chromatin with ncRNAs that silence gene expression by MeCP2. This is highlighted by the chromatinization of the norepinephrine transporter (*NET*) gene by MeCP2 in postural tachycardia syndrome (Khan et al., 2017b). Bisulfite sequencing studies in mouse and human cells show *NET* silencing by MeCP2 independent of CGI methylation changes (Harikrishnan et al., 2010; Bayles et al., 2012). Paradoxical to previous knowledge and against the paradigm at the time, these studies showed that altered chromatin states remodeled by helicase proteins together with MeCP2 serve to autonomously silence *NET* expression. To assess the impact of *NET* chromatinization, a protocol was developed to capture RNA-isolated chromatin followed by deep sequencing. *NET*-interacting RNAs identified *let-7i* as a prime target of MeCP2 (Khan et al., 2017b). At the molecular level, these studies support the view that DNA helicase or ATPase proteins connect ncRNAs and HDAC activity either to suppress gene transcription (Khan et al., 2017a) or to regulate chromatin architecture critical to the nuclear functions associated with gene control.

The regulatory capacity of MeCP2 to co-exist with distinct components on CG methylation sites may be exploited to connect otherwise dipartite regulatory pathways. Here, we report the myocardium-specific lncRNA, *Mhrt*, as a target for MeCP2 recognizing RNA methylation and regulating sex-specific expression of *pri-miR-208b* in the female heart. Binding studies show that the affinity of *Mhrt* RNAmer for MeCP2 is dependent on methylation at CG18, implicating probable role in gene regulation. Therefore, this study is potentially original. We have identified MeCP2 as a physiological target for a cardiac-specific lncRNA. Because methylation of the *Mhrt* lncRNA at CG18 is a substrate for MeCP2, we hypothesize that this affinity for methylated RNA safeguards sex-based cardiac gene suppression.

Recent transcriptome studies have shown widespread RNA methylation in mRNAs and lncRNAs; however, RNA methylation is less abundant than DNA methylation (Squires et al., 2012). Furthermore, RNA methylation at cytosine sites have been shown to influence post-transcriptional gene regulation (Amort et al., 2017; Yang et al., 2017; Aguilo et al., 2016; Shafik et al., 2016; Zhao et al., 2017). In our study, we observed

RNA methylation of *Mhrt* from 25% bisulfite-sequenced clones in the female heart. This resembles the observed frequencies of RNA methylation for the lncRNAs, *HOTAIR* and *XIST* (Schaefer et al., 2009; Amort et al., 2013). Indeed, low-level methylation of *XIST* serves to functionally distinguish methylated from unmethylated versions that bind chromatin-modifying enzymes such as EZH2 and PRC2. In that study (Amort et al., 2013), the reported frequency of *XIST* methylation was approximately 20%. In another study, low-frequency RNA methylation was also observed at specific CG sites in tRNAs (Schaefer et al., 2009). Based on our experimental observations in the female heart we postulate that the affinity of MeCP2 on methylated *Mhrt* could serve to target specific CG sites for gene regulation.

Although the above example clearly indicates that *XIST* methylation influences the interaction of polycomb-group proteins such as EZH2, their effectiveness to bind chromatinized templates is also subject to histone modifications. Indeed, chromatin content as well as loading of specific co-regulatory complexes serve to integrate regional structures to regulate transcriptional events. For example, in cardiac hypertrophy the activation of α-*MHC* and coordinated suppression of β-*MHC* events are mediated by direct interaction of the *pri-miR-208b* lncRNA to the intergenic bdP (Mathiyalagan et al., 2014b). Specifically, α/β-*MHC* transcriptional responses are regulated by the EZH2/*pri-miR-208b* co-repressive complex to form a suppressive environment at the bdP together with the SWI/SNF chromatin-remodeling determinant Brg1. These distinct changes to the intergenic region mean enhanced H3K27me3 by EZH2 and reduced gene-permissive marks such as H3K4me3 and H3K9/14ac. Thus, we postulate that the importance of sex-based *Mhrt* methylation may serve as an effective regulator of *pri-miR-208b* gene expression for maintaining homeostatic transcriptional expression in the adult heart and serve to integrate these events in pathological remodeling of ventricular hypertrophy.

Limitations of the Study

Although the properties of MeCP2 affinity with methylated *Mhrt* are considered consistent with the idea of sexual dimorphism regulating *pri-miR-208b* expression, this idea has not yet been tested completely. First, sex-specific methylation of the lncRNA *Mhrt* at CG18 in the female heart remains poorly understood. The challenge now is to understand how the cardiovascular phenotype with respect to hormonal regulation could control gene expression and sex differences (Mosca et al., 2011). Second, we also acknowledge that although this study emphasizes RNA methylation-dependent MeCP2 binding in the heart, it now becomes apparent that methylation of other RNA sites could also be prime candidates for default repression by methylation that need to be tested. Although lncRNAs interacting with DNMTs have been documented to regulate DNA methylation (Di Ruscio et al., 2013), our results show proof of concept that *Mhrt* methylation is a target for MeCP2 to regulate *pri-miR-208b* expression independent of differential DNA methylation. Furthermore, although we appreciate that CG18 methylation of *Mhrt* was not critically tested using animal models of cardiac disease, future studies should allow us to test the generalizability of site-specific RNA methylation and protein interaction using *in vitro* and *in vivo* experimental models.

METHODS

All methods can be found in the accompanying Transparent Methods supplemental file.

SUPPLEMENTAL INFORMATION

Supplemental Information can be found online at https://doi.org/10.1016/j.isci.2019.06.031.

ACKNOWLEDGMENTS

Professor Assam El-Osta is a National Health and Medical Research Council (NHMRC) Senior Research Fellow (1154650), and this work is supported by NHMRC-NSFC International Joint Grant (1113188 and 15070000000090844) and NHMRC grants (1032687 and 526635).

AUTHOR CONTRIBUTIONS

H.K.N., J.O., and P.M. performed the study design, validation, and data representation; H.K.N. and P.M. performed the ChIP, bisulfite sequencing, and *in vitro* binding assays; J.O. cloned and synthesized Mhrt full-length transcript; J.O., P.M., and A.W.K. prepared the figures; S.A.J., G.S., and X.-J.D. were involved in mouse tissue handling and resources; M.Z. analyzed bisulfite sequencing data; and A.E.-O. was involved in the design, supervision, funding, and writing of the manuscript, which has been reviewed and edited by the co-authors.

DECLARATION OF INTERESTS

The authors declare there is no competing interests.

Received: April 30, 2018
Revised: May 13, 2019
Accepted: June 20, 2019
Published: July 26, 2019

REFERENCES

Aguilo, F., Li, S., Balasubramaniyan, N., Sancho, A., Benko, S., Zhang, F., Vashisht, A., Rengasamy, M., Andino, B., Chen, C.H., et al. (2016). Deposition of 5-methylcytosine on enhancer RNAs enables the coactivator function of PGC-1alpha. Cell Rep. *14*, 479–492.

Amort, T., Rieder, D., Wille, A., Khokhlova-Cubberley, D., Riml, C., Trixl, L., Jia, X.Y., Micura, R., and Lusser, A. (2017). Distinct 5-methylcytosine profiles in poly(A) RNA from mouse embryonic stem cells and brain. Genome Biol. *18*, 1.

Amort, T., Souliere, M.F., Wille, A., Jia, X.Y., Fiegl, H., Worle, H., Micura, R., and Lusser, A. (2013). Long non-coding RNAs as targets for cytosine methylation. RNA Biol. *10*, 1003–1008.

Anderson, K.M., Anderson, D.M., Mcanally, J.R., Shelton, J.M., Bassel-Duby, R., and Olson, E.N. (2016). Transcription of the non-coding RNA upperhand controls Hand2 expression and heart development. Nature *539*, 433–436.

Bayles, R., Harikrishnan, K.N., Lambert, E., Baker, E.K., Agrotis, A., Guo, L., Jowett, J.B., Esler, M., Lambert, G., and El-Osta, A. (2012). Epigenetic modification of the norepinephrine transporter gene in postural tachycardia syndrome. Arterioscler. Thromb. Vasc. Biol. *32*, 1910–1916.

Bird, A.P., and Wolffe, A.P. (1999). Methylation-induced repression–belts, braces, and chromatin. Cell *99*, 451–454.

Carninci, P., Sandelin, A., Lenhard, B., Katayama, S., Shimokawa, K., Ponjavic, J., Semple, C.A., Taylor, M.S., Engstrom, P.G., Frith, M.C., et al. (2006). Genome-wide analysis of mammalian promoter architecture and evolution. Nat. Genet. *38*, 626–635.

Cheng, T.L., Wang, Z., Liao, Q., Zhu, Y., Zhou, W.H., Xu, W., and Qiu, Z. (2014). MeCP2 suppresses nuclear microRNA processing and dendritic growth by regulating the DGCR8/Drosha complex. Dev. Cell *28*, 547–560.

Chizzonite, R.A., and Zak, R. (1984). Regulation of myosin isoenzyme composition in fetal and neonatal rat ventricle by endogenous thyroid hormones. J. Biol. Chem. *259*, 12628–12632.

Di Ruscio, A., Ebralidze, A.K., Benoukraf, T., Amabile, G., Goff, L.A., Terragni, J., Figueroa, M.E., De Figueiredo Pontes, L.L., Alberich-Jorda, M., Zhang, P., et al. (2013). DNMT1-interacting RNAs block gene-specific DNA methylation. Nature *503*, 371–376.

Flynn, J., Glickman, J.F., and Reich, N.O. (1996). Murine DNA cytosine-C5 methyltransferase: pre-steady- and steady-state kinetic analysis with regulatory DNA sequences. Biochemistry *35*, 7308–7315.

Frey, N., and Olson, E.N. (2003). Cardiac hypertrophy: the good, the bad, and the ugly. Annu. Rev. Physiol. *65*, 45–79.

Grote, P., Wittler, L., Hendrix, D., Koch, F., Wahrisch, S., Beisaw, A., Macura, K., Blass, G., Kellis, M., Werber, M., and Herrmann, B.G. (2013). The tissue-specific lncRNA Fendrr is an essential regulator of heart and body wall development in the mouse. Dev. Cell *24*, 206–214.

Guerra, S., Leri, A., Wang, X., Finato, N., Di Loreto, C., Beltrami, C.A., Kajstura, J., and Anversa, P. (1999). Myocyte death in the failing human heart is gender dependent. Circ. Res. *85*, 856–866.

Haddad, F., Bodell, P.W., Qin, A.X., Giger, J.M., and Baldwin, K.M. (2003). Role of antisense RNA in coordinating cardiac myosin heavy chain gene switching. J. Biol. Chem. *278*, 37132–37138.

Han, P., Li, W., Lin, C.H., Yang, J., Shang, C., Nurnberg, S.T., Jin, K.K., Xu, W., Lin, C.Y., Lin, C.J., et al. (2014). A long noncoding RNA protects the heart from pathological hypertrophy. Nature *514*, 102–106.

Harikrishnan, K.N., Bayles, R., Ciccotosto, G.D., Maxwell, S., Cappai, R., Pelka, G.J., Tam, P.P., Christodoulou, J., and El-Osta, A. (2010). Alleviating transcriptional inhibition of the norepinephrine slc6a2 transporter gene in depolarized neurons. J. Neurosci. *30*, 1494–1501.

Harikrishnan, K.N., Chow, M.Z., Baker, E.K., Pal, S., Bassal, S., Brasacchio, D., Wang, L., Craig, J.M., Jones, P.L., Sif, S., and El-Osta, A. (2005). Brahma links the SWI/SNF chromatin-remodeling complex with MeCP2-dependent transcriptional silencing. Nat. Genet. *37*, 254–264.

Hwang, C.K., Song, K.Y., Kim, C.S., Choi, H.S., Guo, X.H., Law, P.Y., Wei, L.N., and Loh, H.H. (2009). Epigenetic programming of mu-opioid receptor gene in mouse brain is regulated by MeCP2 and Brg1 chromatin remodelling factor. J. Cell Mol. Med. *13*, 3591–3615.

Izumo, S., Lompre, A.M., Matsuoka, R., Koren, G., Schwartz, K., Nadal-Ginard, B., and Mahdavi, V. (1987). Myosin heavy chain messenger RNA and protein isoform transitions during cardiac hypertrophy. Interaction between hemodynamic and thyroid hormone-induced signals. J. Clin. Invest. *79*, 970–977.

Jeffery, L., and Nakielny, S. (2004). Components of the DNA methylation system of chromatin control are RNA-binding proteins. J. Biol. Chem. *279*, 49479–49487.

Khan, A.W., Corcoran, S.J., Esler, M., and El-Osta, A. (2017a). Epigenomic changes associated with impaired norepinephrine transporter function in postural tachycardia syndrome. Neurosci. Biobehav. Rev. *74*, 342–355.

Khan, A.W., Ziemann, M., Corcoran, S.J., K, N.H., Okabe, J., Rafehi, H., Maxwell, S.S., Esler, M.D., and El-Osta, A. (2017b). NET silencing by let-7i in postural tachycardia syndrome. JCI Insight *2*, e90183.

Khan, A.W., Ziemann, M., Rafehi, H., Maxwell, S., Ciccotosto, G.D., and El-Osta, A. (2017c). MeCP2 interacts with chromosomal microRNAs in brain. Epigenetics *12*, 1028–1037.

Klattenhoff, C.A., Scheuermann, J.C., Surface, L.E., Bradley, R.K., Fields, P.A., Steinhauser, M.L., Ding, H., Butty, V.L., Torrey, L., Haas, S., et al. (2013). Braveheart, a long noncoding RNA required for cardiovascular lineage commitment. Cell *152*, 570–583.

Kurian, J.R., Olesen, K.M., and Auger, A.P. (2010). Sex differences in epigenetic regulation of the estrogen receptor-alpha promoter within the developing preoptic area. Endocrinology *151*, 2297–2305.

Lee, H.C., Aalto, A.P., Yang, Q., Chang, S.S., Huang, G., Fisher, D., Cha, J., Poranen, M.M., Bamford, D.H., and Liu, Y. (2010). The DNA/RNA-dependent RNA polymerase QDE-1 generates aberrant RNA and dsRNA for RNAi in a process requiring replication protein A and a DNA helicase. PLoS Biol. *8*, https://doi.org/10.1371/journal.pbio.1000496.

Lewis, J.D., Meehan, R.R., Henzel, W.J., Maurer-Fogy, I., Jeppesen, P., Klein, F., and Bird, A. (1992). Purification, sequence, and cellular localization of a novel chromosomal protein that binds to methylated DNA. Cell *69*, 905–914.

Litten, R.Z., 3rd, Martin, B.J., Low, R.B., and Alpert, N.R. (1982). Altered myosin isozyme patterns from pressure-overloaded and thyrotoxic hypertrophied rabbit hearts. Circ. Res. *50*, 856–864.

Lompre, A.M., Mercadier, J.J., Wisnewsky, C., Bouveret, P., Pantaloni, C., D'albis, A., and Schwartz, K. (1981). Species- and age-dependent changes in the relative amounts of cardiac myosin isoenzymes in mammals. Dev. Biol. *84*, 286–290.

Lompre, A.M., Nadal-Ginard, B., and Mahdavi, V. (1984). Expression of the cardiac ventricular alpha- and beta-myosin heavy chain genes is developmentally and hormonally regulated. J. Biol. Chem. *259*, 6437–6446.

Lompre, A.M., Schwartz, K., D'albis, A., Lacombe, G., Van Thiem, N., and Swynghedauw, B. (1979). Myosin isoenzyme redistribution in chronic heart overload. Nature *282*, 105–107.

Long, S.W., Ooi, J.Y., Yau, P.M., and Jones, P.L. (2011). A brain-derived MeCP2 complex supports a role for MeCP2 in RNA processing. Biosci. Rep. *31*, 333–343.

Lujambio, A., and Esteller, M. (2007). CpG island hypermethylation of tumor suppressor microRNAs in human cancer. Cell Cycle *6*, 1455–1459.

Maas, A.H., and Appelman, Y.E. (2010). Gender differences in coronary heart disease. Neth. Heart J. *18*, 598–602.

Mahdavi, V., Chambers, A.P., and Nadal-Ginard, B. (1984). Cardiac alpha- and beta-myosin heavy chain genes are organized in tandem. Proc. Natl. Acad. Sci. U S A *81*, 2626–2630.

Mahdavi, V., Periasamy, M., and Nadal-Ginard, B. (1982). Molecular characterization of two myosin heavy chain genes expressed in the adult heart. Nature *297*, 659–664.

Mathiyalagan, P., Keating, S.T., Du, X.J., and El-Osta, A. (2014a). Interplay of chromatin modifications and non-coding RNAs in the heart. Epigenetics *9*, 101–112.

Mathiyalagan, P., Okabe, J., Chang, L., Su, Y., Du, X.J., and El-Osta, A. (2014b). The primary microRNA-208b interacts with Polycomb-group protein, Ezh2, to regulate gene expression in the heart. Nucleic Acids Res. *42*, 790–803.

Maxwell, S.S., Pelka, G.J., Tam, P.P., and El-Osta, A. (2013). Chromatin context and ncRNA highlight targets of MeCP2 in brain. RNA Biol. *10*, 1741–1757.

Mayer, S.C., Gilsbach, R., Preissl, S., Monroy Ordonez, E.B., Schnick, T., Beetz, N., Lother, A., Rommel, C., Ihle, H., et al. (2015). Adrenergic repression of the epigenetic reader MeCP2 facilitates cardiac adaptation in chronic heart failure. Circ. Res. *117*, 622–633.

Meehan, R.R., Lewis, J.D., and Bird, A.P. (1992). Characterization of MeCP2, a vertebrate DNA binding protein with affinity for methylated DNA. Nucleic Acids Res. *20*, 5085–5092.

Mercer, T.R., and Mattick, J.S. (2013). Structure and function of long noncoding RNAs in epigenetic regulation. Nat. Struct. Mol. Biol. *20*, 300–307.

Micheletti, R., Plaisance, I., Abraham, B.J., Sarre, A., Ting, C.C., Alexanian, M., Maric, D., Maison, D., Nemir, M., Young, R.A., et al. (2017). The long noncoding RNA Wisper controls cardiac fibrosis and remodeling. Sci. Transl. Med. *9*, https://doi.org/10.1126/scitranslmed.aai9118.

Monteys, A.M., Spengler, R.M., Wan, J., Tecedor, L., Lennox, K.A., Xing, Y., and Davidson, B.L. (2010). Structure and activity of putative intronic miRNA promoters. RNA *16*, 495–505.

Mosca, L., Barrett-Connor, E., and Wenger, N.K. (2011). Sex/gender differences in cardiovascular disease prevention: what a difference a decade makes. Circulation *124*, 2145–2154.

Nan, X., Campoy, F.J., and Bird, A. (1997). MeCP2 is a transcriptional repressor with abundant binding sites in genomic chromatin. Cell *88*, 471–481.

Nan, X., Hou, J., Maclean, A., Nasir, J., Lafuente, M.J., Shu, X., Kriaucionis, S., and Bird, A. (2007). Interaction between chromatin proteins MECP2 and ATRX is disrupted by mutations that cause inherited mental retardation. Proc. Natl. Acad. Sci. U S A *104*, 2709–2714.

Nan, X., Tate, P., Li, E., and Bird, A. (1996). DNA methylation specifies chromosomal localization of MeCP2. Mol. Cell Biol. *16*, 414–421.

Noh, K.M., Hwang, J.Y., Follenzi, A., Athanasiadou, R., Miyawaki, T., Greally, J.M., Bennett, M.V., and Zukin, R.S. (2012). Repressor element-1 silencing transcription factor (REST)-dependent epigenetic remodeling is critical to ischemia-induced neuronal death. Proc. Natl. Acad. Sci. U S A *109*, E962–E971.

Ooi, L., and Wood, I.C. (2007). Chromatin crosstalk in development and disease: lessons from REST. Nat. Rev. Genet. *8*, 544–554.

Ounzain, S., Micheletti, R., Arnan, C., Plaisance, I., Cecchi, D., Schroen, B., Reverter, F., Alexanian, M., Gonzales, C., Ng, S.Y., et al. (2015). CARMEN, a human super enhancer-associated long noncoding RNA controlling cardiac specification, differentiation and homeostasis. J. Mol. Cell Cardiol. *89*, 98–112.

Ozsolak, F., Poling, L.L., Wang, Z.X., Liu, H., Liu, X.S., Roeder, R.G., Zhang, X.M., Song, J.S., and Fisher, D.E. (2008). Chromatin structure analyses identify miRNA promoters. Genes Dev. *22*, 3172–3183.

Place, R.F., Li, L.C., Pookot, D., Noonan, E.J., and Dahiya, R. (2008). MicroRNA-373 induces expression of genes with complementary promoter sequences. Proc. Natl. Acad. Sci. U S A *105*, 1608–1613.

Ratnu, V.S., Emami, M.R., and Bredy, T.W. (2017). Genetic and epigenetic factors underlying sex differences in the regulation of gene expression in the brain. J. Neurosci. Res. *95*, 301–310.

Robertson, K.D., Ait-Si-Ali, S., Yokochi, T., Wade, P.A., Jones, P.L., and Wolffe, A.P. (2000). DNMT1 forms a complex with Rb, E2F1 and HDAC1 and represses transcription from E2F-responsive promoters. Nat. Genet. *25*, 338–342.

Schaefer, M., Pollex, T., Hanna, K., and Lyko, F. (2009). RNA cytosine methylation analysis by bisulfite sequencing. Nucleic Acids Res. *37*, e12.

Schmitz, K.M., Mayer, C., Postepska, A., and Grummt, I. (2010). Interaction of noncoding RNA with the rDNA promoter mediates recruitment of DNMT3b and silencing of rRNA genes. Genes Dev. *24*, 2264–2269.

Schonrock, N., Harvey, R.P., and Mattick, J.S. (2012). Long noncoding RNAs in cardiac development and pathophysiology. Circ. Res. *111*, 1349–1362.

Shafik, A., Schumann, U., Evers, M., Sibbritt, T., and Preiss, T. (2016). The emerging epitranscriptomics of long noncoding RNAs. Biochim. Biophys. Acta *1859*, 59–70.

Simpson, P.C. (2015). A New pathway for sympathetic cardioprotection in heart failure. Circ. Res. *117*, 592–595.

Squires, J.E., Patel, H.R., Nousch, M., Sibbritt, T., Humphreys, D.T., Parker, B.J., Suter, C.M., and Preiss, T. (2012). Widespread occurrence of 5-methylcytosine in human coding and non-coding RNA. Nucleic Acids Res. *40*, 5023–5033.

Trinklein, N.D., Aldred, S.F., Hartman, S.J., Schroeder, D.I., Otillar, R.P., and Myers, R.M. (2004). An abundance of bidirectional promoters in the human genome. Genome Res. *14*, 62–66.

Tsang, J., Zhu, J., and Van Oudenaarden, A. (2007). MicroRNA-mediated feedback and feedforward loops are recurrent network motifs in mammals. Mol. Cell *26*, 753–767.

van Rooij, E., Quiat, D., Johnson, B.A., Sutherland, L.B., Qi, X.X., Richardson, J.A., Kelm, R.J., and Olson, E.N. (2009). A family of microRNAs encoded by myosin genes governs myosin expression and muscle performance. Dev. Cell *17*, 662–673.

Viereck, J., Kumarswamy, R., Foinquinos, A., Xiao, K., Avramopoulos, P., Kunz, M., Dittrich, M., Maetzig, T., Zimmer, K., Remke, J., et al. (2016). Long noncoding RNA Chast promotes cardiac remodeling. Sci. Transl. Med. *8*, 326ra22.

Wade, P.A., Jones, P.L., Vermaak, D., Veenstra, G.J., Imhof, A., Sera, T., Tse, C., Ge, H., Shi, Y.B., Hansen, J.C., and Wolffe, A.P. (1998). Histone deacetylase directs the dominant silencing of transcription in chromatin: association with MeCP2 and the Mi-2 chromodomain SWI/SNF ATPase. Cold Spring Harb. Symp. Quant. Biol. *63*, 435–445.

Wang, K., Liu, F., Zhou, L.Y., Long, B., Yuan, S.M., Wang, Y., Liu, C.Y., Sun, T., Zhang, X.J., and Li, P.F. (2014). The long noncoding RNA CHRF regulates cardiac hypertrophy by targeting miR-489. Circ. Res. *114*, 1377–1388.

Wang, Z., Zhang, X.J., Ji, Y.X., Zhang, P., Deng, K.Q., Gong, J., Ren, S., Wang, X., Chen, I., Wang, H., et al. (2016). The long noncoding RNA Chaer defines an epigenetic checkpoint in cardiac hypertrophy. Nat. Med. *22*, 1131–1139.

Weinberg, E.O., Thienelt, C.D., Katz, S.E., Bartunek, J., Tajima, M., Rohrbach, S., Douglas, P.S., and Lorell, B.H. (1999). Gender differences in molecular remodeling in pressure overload hypertrophy. J. Am. Coll. Cardiol. *34*, 264–273.

Yang, X., Yang, Y., Sun, B.F., Chen, Y.S., Xu, J.W., Lai, W.Y., Li, A., Wang, X., Bhattarai, D.P., Xiao, W., et al. (2017). 5-methylcytosine promotes mRNA export - NSUN2 as the methyltransferase and ALYREF as an m(5)C reader. Cell Res. *27*, 606–625.

Young, J.I., Hong, E.P., Castle, J.C., Crespo-Barreto, J., Bowman, A.B., Rose, M.F., Kang, D., Richman, R., Johnson, J.M., Berget, S., and Zoghbi, H.Y. (2005). Regulation of RNA splicing by the methylation-dependent transcriptional repressor methyl-CpG binding protein 2. Proc. Natl. Acad. Sci. U S A *102*, 17551–17558.

Zhao, B.S., Roundtree, I.A., and He, C. (2017). Post-transcriptional gene regulation by mRNA modifications. Nat. Rev. Mol. Cell Biol. *18*, 31–42.

Zhong, Y., Reiser, P.J., and Matlib, M.A. (2003). Gender differences in myosin heavy chain-beta and phosphorylated phospholamban in diabetic rat hearts. Am. J. Physiol. Heart Circ. Physiol. *285*, H2688–H2693.

ISCI, Volume *17*

Supplemental Information

Sex-Based *Mhrt* Methylation Chromatinizes MeCP2 in the Heart

Harikrishnan K.N., Jun Okabe, Prabhu Mathiyalagan, Abdul Waheed Khan, Sameer A. Jadaan, Gulcan Sarila, Mark Ziemann, Ishant Khurana, Scott S. Maxwell, Xiao-Jun Du, and Assam El-Osta

Transparent Methods

Preparation of mouse heart left ventricular tissue

Hearts isolated from 6-weeks old C57BL/6 male and female mice were used in this study. The ventricular base was carefully dissected from the atrial compartment using sterile iris scissors. Excessive blood from ventricles was removed by washing with ice-cold PBS. Left ventricular (LV) and right ventricular (RV) tissues were then carefully dissected by cutting down the tricuspid valve interface.

Total RNA extraction and qRT-PCR

LVs isolated from male and female mice were diced and suspended in ice-cold PBS. Total RNA was isolated using Trizol (Invitrogen) reagent by following the manufacturer's protocol. For first strand cDNA synthesis, 1 μg of total RNA was reverse transcribed using High capacity cDNA Reverse Transcription Kit (Life Technologies). Real-time PCR (qPCR) was performed using the ABI Prism 7500 instrument and template amplification was assessed by melt-curve analysis. Gene expression data between male and female LVs are expressed relative to endogenous GAPDH. Oligonucleotide sequences used for qPCR are listed in (Table 1). For strand-specific quantitative reverse transcriptase-polymerase chain reaction (qRT-PCR) of *MHC* genes, forward and reverse primers were included in separate reactions, and cDNA synthesis was performed at 60°C using Thermoscript cDNA preparation system (Invitrogen) and real-time quantification was performed using Fast SYBR-Green qPCR system (Applied Biosystems). To ensure strand-specific cDNA synthesis, negative primer controls and negative enzyme controls were included and assessed for negligible non-specific amplification. Samples analyzed included $n \geq 5$ in male and female and are normalized against GAPDH gene and the data are represented as mean ±SEM.

Chromatin Immunoprecipitation (ChIP)

Male and female LVs were finely chopped in to tiny pieces in ice-cold PBS and chromatin was fixed immediately by incubation for 10 minutes at room temperature using 1% formaldehyde. Excessive formaldehyde was quenched using 0.1M glycine by incubation for 10 minutes at room temperature. Tissues were washed with ice-cold PBS to remove residual glycine, resuspended in fresh ice-cold PBS and homogenized to a clear solution in presence of protease inhibitor cocktail. Homogenates were incubated on ice for 30 minutes in SDS lysis buffer containing 1% SDS, 10mM EDTA, 50mM Tris-HCl, pH 8, and protease inhibitor cocktail. Lysates were separated into 300 µL aliquots and sonication of chromatin was achieved using the bioruptor (Diagenode, Belgium) with constant power settings. Soluble chromatin fractions were collected by centrifugation and chromatin shearing was ensured to be in the range of 300-500bp fragments using MultiNA capillary electrophoresis system (Shimadzu). Approximately 10 µg of chromatin was suspended in ChIP dilution buffer (0.01% SDS, 1.1% Triton X-100, 1.2 mM EDTA, 16.7 mM Tris-HCl pH 8, 167 mM NaCl) and immunopurification was carried out using antibodies specific to HDAC2 (3159, Sigma), MeCP2 (9317, Sigma), REST (07-579, Upstate), MBD1 (ab2846, Abcam), MBD2 (ab38646, Abcam), MBD3 (ab157464, Abcam). Non-specific IgG was incubated simultaneously to each reaction as control. The antibody-bound chromatin fraction was precipitated using dynabeads coated with protein A/G (Invitrogen). Antibody-chromatin-protein A/G conjugates were washed sequentially with low salt buffer, high salt buffer, lithium chloride, Tris-EDTA and Tris-EDTA + 0.01% SDS. Formaldehyde reverse crosslinking was carried out using ChIP elution buffer (20 mM Tris-HCl pH7.5, 5 mM EDTA, 50 mM NaCl, 1% SDS) and incubation in presence of proteinase K (Invitrogen) for 2 hours at 62^{o}C in a thermomixer at 1400rpm (Eppendorf). Input chromatin was included at this reverse crosslinking stage. ChIP enriched DNA was purified using DNA binding columns according to the manufacturer's protocol (Nucleospin, Macherey-Nagel) and eluted in nuclease free water. Relative enrichment of DNA in input, ChIP and IgG samples was quantified using Fast SYBR Green qPCR system (Applied Biosystems). Primer sequences used to amplify the cardiac myosin heavy chain genomic sequences

are provided in Table 2. Percentage input (% input) was calculated for each ChIP experiment, and results are expressed as relative to input chromatin between male and female LV tissues. Samples were analyzed as n=4 for male and female and the percentage of input was calculated, and the data are presented as mean ±SEM.

RNase treatment of immunopurified chromatin

ChIP using anti-MeCP2 antibody from male and female LV was carried out as described above. The protein A/G bound conjugates were resuspended in 100 µl of either RNase A reaction buffer (10 mM Tris-HCl, 300 mM NaCl, 5 mM EDTA, pH 7.5) or RNase H reaction buffer (50 mM Tris-HCl, 75 mM KCl, 3 mM MgCl2, 10 mM DTT, pH 8.0). RNase A (Sigma), RNase H and RNase V1 (New England Biolabs) were added to corresponding tubes and incubated at 37^{o}C for one hour. Sequential washing of beads was carried out as described above. DNA was purified using DNA binding columns according to the manufacturer's protocol (Nucleospin, Macherey-Nagel) and eluted in nuclease free water. Amplification of genomic DNA was carried out using real time qPCR and enrichment of DNA sequences were calculated as % input and statistics was obtained between control, RNase treated samples as described above.

RNA Chromatin Immunoprecipitation (RNA-ChIP)

Male and female LV chromatin was prepared by the lysis of tissues in SDS buffer and shearing by sonication to optimal size (300-500 bp long). To ensure RNA integrity and to protect chromatin-bound RNA from RNase degradation, only freshly prepared buffers containing RNase inhibitors were used. Tissue homogenates were sonicated in the size optimized for RNA ChIP and residual DNA from sheared chromatin was removed by mild DNase treatment. Immunoprecipitation of chromatin was carried out at 4°C overnight using anti-MeCP2 antibody (9317, Sigma) and a control IgG antibody. Chromatin-bound RNA was purified using RNeasy columns (Qiagen) followed by removal of residual DNA (Ambion). Relative enrichment of *Mhrt* was assessed using SYBR Green qPCR and

chromatin binding was expressed relative to input (% Input) chromatin in male and female LV tissues. Samples were analysed as n=6 for male and female and the percentage of input was calculated, and the data are presented as mean ±SEM.

Genomic DNA methylation and sequencing analysis

About 500 ng of genomic DNA isolated from male and female LV tissues were used per bisulphite reaction. Bisulphite conversion was performed according to the manufacturers protocol (EpiTect, Qiagen). The genomic sequence comprising MHC CpG island was amplified using the primers as listed in Table 3. Between 5 and 50 ng of amplicon DNA was used to prepare sequencing libraries using the NEBNext® DNA Library Prep Reagent Set for Illumina (New England Biolabs, NEB). Enzymatic reaction cleanups were performed using QIAquick PCR Purification Kit (Qiagen). Size selection of the libraries was performed by agarose gel excision and QIAquick Gel Extraction Kit (Qiagen). Each amplicon was given a unique barcode using the NEBNext® Multiplex Oligos for Illumina (Index Primers Set 1 and Set 2) (NEB). Library DNA was quantified on the MultiNA bioanalyzer (Shimadzu) and pooled in equimolar amounts. Pooled library DNA was diluted to 4 nM and underwent sequencing on the MiSeq system using MiSeq Reagent Kit v2 500 cycle (Illumina) at a concentration of 8 pM.

***In vitro* DNA/RNA/Protein binding assay**

Full-length *Mhrt* transcript was amplified using the primers (Fw: AAGAGCCCTACAGTCTGATGAACA / Rev: CCTTTACTCTCTGCTTCATTGCCT) and cloned into pCRII-TOPO cloning vector (Invitrogen). Full-length *Mhrt* RNA was synthesized by the HiScribe T7 Quick Kit (NEB). *In vitro* dsDNA/RNA binding assay was performed as described previously (Mathiyalagan et al., 2014). The dsDNA/RNA hybrids (*Mhrt* full length, CG8-9, CG17-19 or methylated CG17-19) were incubated with rMeCP2 protein at 37°C for 30 mins in the presence or absence of RNaseH. This complex was immunopurified with MeCP2 antibody (9317, Sigma) in

the presence of protein A dynabeads for 30 mins at 25°C (Supplemental Fig. S4). DNA was purified using DNA binding columns according to the manufacturer's protocol (Nucleospin, Macherey-Nagel). Relative enrichment of input DNA and the bound samples were amplified by qPCR to check the binding of MeCP2 to the promoter DNA of pri-miRNA-208b.

RNA methylation analysis

Total RNA extracted from male and female LV was used for 5-methyl cytosine (5-mC) methylation analysis using EZ RNA Methylation Kit (Zymo Research). 1 μg RNA was subjected to deamination. Removal of bisulphite, desulphonation and RNA washing were performed in RNA spin columns as recommended by the manufacturer. Deaminated RNA was eluted in Nuclease-free water and used for cDNA conversion using High Capacity cDNA Reverse Transcription Kit (Life Technologies). Methylation efficiency and analysis in male and female LV RNA extract was confirmed using primers specific for deaminated sequences in mAsp tRNA as a positive control (Table 3). To assess bisulphite converted RNA, *Mhrt* was amplified using five individual primer pairs denoted as primers A-E listed in Table 3. This is because bisulphite-qPCR facilitates efficient amplification of shorter amplicons of the transcript. Following bisulphite conversion, we assessed 6-8 clones of each amplicon (i.e. for each of the five regions designated A-E) using Sanger sequencing. Therefore 30-40 clones per mouse combining the five regions designated A-E were analysed. To distinguish male and female differences in *Mhrt* methylation, we examined n=5 mice.

Methylation of synthetic oligomers and *Mhrt*:MeCP2 binding assay

Biotin-tagged three synthetic RNA oligomers of 45 nucleotides in length (Fig. 4D) were used in this experiment (Sigma). RNA oligomers were modified for CG sequences as described in the text. For in vitro methylation, oligomers were methylated using *Sss1* methylase (NEB) according to the manufacturers protocol. *Mhrt* oligomer, diluted stock of SAM (S-Adenosyl methionine) and *Sss1* methylase (4U/μl) were incubated at 37°C for 1 hr. The reaction was stopped by heating at 65°C for

20 mins. In vitro binding assay was carried out in the presence of recombinant proteins MeCP2 or SET7 (negative control). The methylated and unmethylated probes were incubated in the presence of a binding buffer (20mM Tris-HCl, 180mM NaCl, 0.1% NP-40, 1.5mM MgCl2 and 13.2% glycerol) with rMeCP2 or rSET7 proteins for 30 mins at 25°C. Protein:RNA complexes were immunopurified using streptavidin beads and treated for +/- RNAse for 10 mins at 37°C followed by detection by western blotting using MeCP2 (9317, Sigma) and SET7 (NB100-93288, Novus Biologicals) antibodies and quantitation was performed by Odyssey assay. All the assays were done in triplicates and the quantitation was done by normalizing against the input protein.

Data analysis and statistics

Data are presented as ±SEM in each group. All data were evaluated with a two-tailed, unpaired Student's t-test. Statistical significance was obtained by comparing male LV and female LV. A value of $P < 0.05$ was considered statistically significant between groups.

References

Mathiyalagan, P., Okabe, J., Chang, L., Su, Y., Du, X.J., and El-Osta, A. (2014). The primary microRNA-208b interacts with Polycomb-group protein, Ezh2, to regulate gene expression in the heart. Nucleic Acids Res *42*, 790-803.

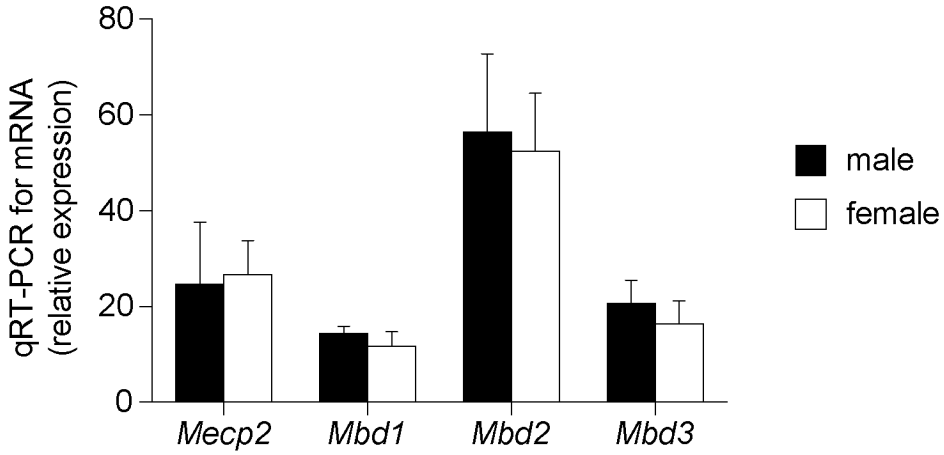

Supplemental Figure S1, related to Figure 2. mRNA expression of methyl CpG binding proteins (*Mecp2*, *Mbd1*, *Mbd2* and *Mbd3*) examined by qRT-PCR. n=5 mice per group. Data are represented as mean ±SEM.

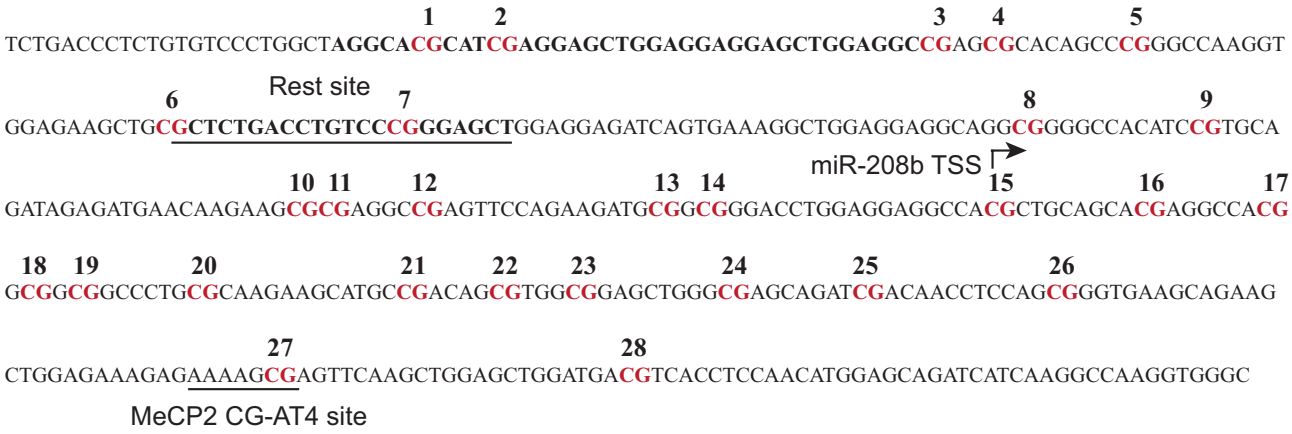

Supplemental Figure S2, related to Figure 3. In silico prediction of transcription factor binding revealed MeCP2 and Rest corepressor complex binding sequences at the CGI within *pri-miR-208b* promoter. Transcription start site is shown here as the TSS.

Predicted secondary structure mouse *Mhrt* lncRNA (minimal free energy)

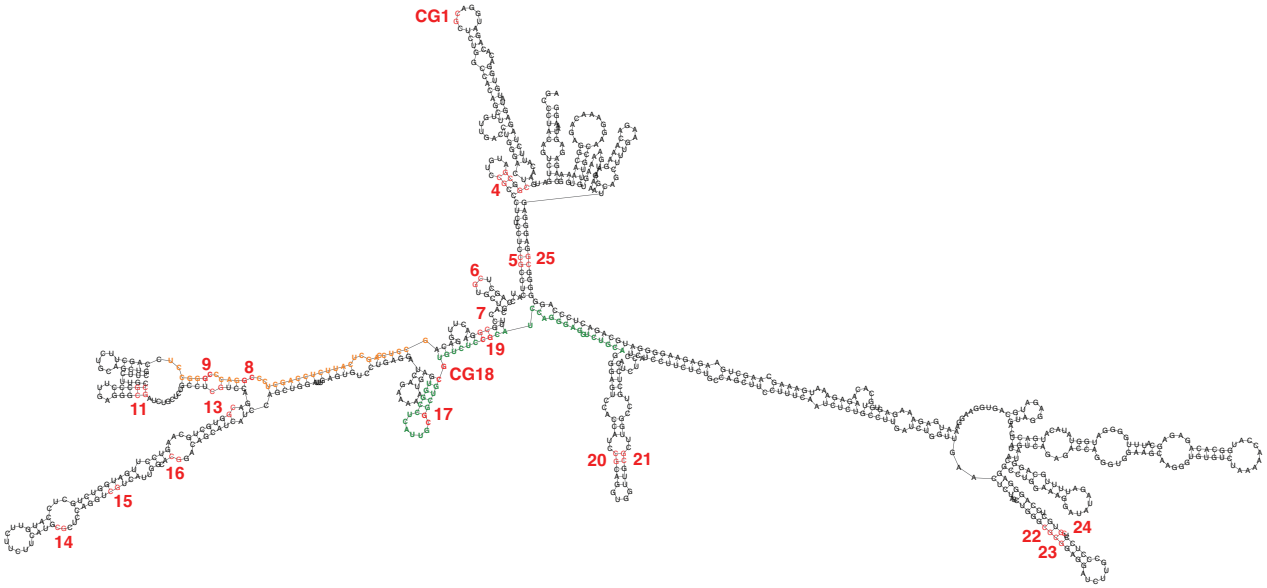

AGCCCTACAGTCTGATGAACATTCTAGAGTATGTGGACACAGATGGACGCTCTGGCCACAGCTTGTTGACCTGGGACTCGGCGATGTCCGCCC
TCTCCTCCGCCTCATCCAGCTCGTGCTGCACCTTGCGGAACTTGGACAGCCTCCAGCTCATTCTCCAGCTCCCGGACCCGGGCCTCCAGCTTC
TGCAGCTGCTTCTTGCCGCCCTTGAGGGCGATCTGCTCTGCCTCGTCCAGACGGTGCTGCAAGTCCTTGATGGTCTGCTCCATGTTCTTCTTC
ATGCGCTCCAGGTCGTCATTGGCACGGACAGCATCATCCAGCTGGATTTGAGTGTCCTGAGGATCAGAAAAATGAGTGGCCTCATTGCGGCTG
CGTGTCTCCGCATCCAGGGAGGTCTGCAGGGAGTCCACCATCCGCAGGTGGTTGCGCTTGGCCTGCTCCATCTCCTCATCCTTCTCTGCCAGC
TTCCTTTCAATCTCTGCCTTGATCTGGTTGAACTCTAGCTGGGCGCGGAGGATCTTGCCCTCCTCGTGCTCCAGGGAGGCCTGGAAAGGATAT
AGATTTTGCAGGCATATAGTCAGAGACCAGGGTGGAAGCAAGGGTGTGTCTAAAAACCATGGCACAGAGAGCATTTGGGGATGGTATACATGA
CTCAGTAGGAGATGCAGTGGAAGGAAATGAGAAAGAGTGTGCACAAGAGAAATGAAAGCAAGCTGAAGAGAAGGGGATGCAGACTCCCAGGGG
GGCGGAGGGAGTCAGCTTTGAAGACAAAGAGGAAAATGAAAAGTGTTGCCAAGGAAACAGAGGCAATGAAGCAGAGAGTAAAGG

Supplemental Figure S3, related to Figure 3C. Illustration of predicted secondary structure of full length *Mhrt* using RNAfold Webserver (http://rna.tbi.univie.ac.at/cgi-bin/RNAWebSuite/RNAfold.cgi). Predicted Mhrt RNA/DNA hybrid sequence at the *pri-miR-208b* promoter shown in orange. The positions of CG dinucleotides shown in red.

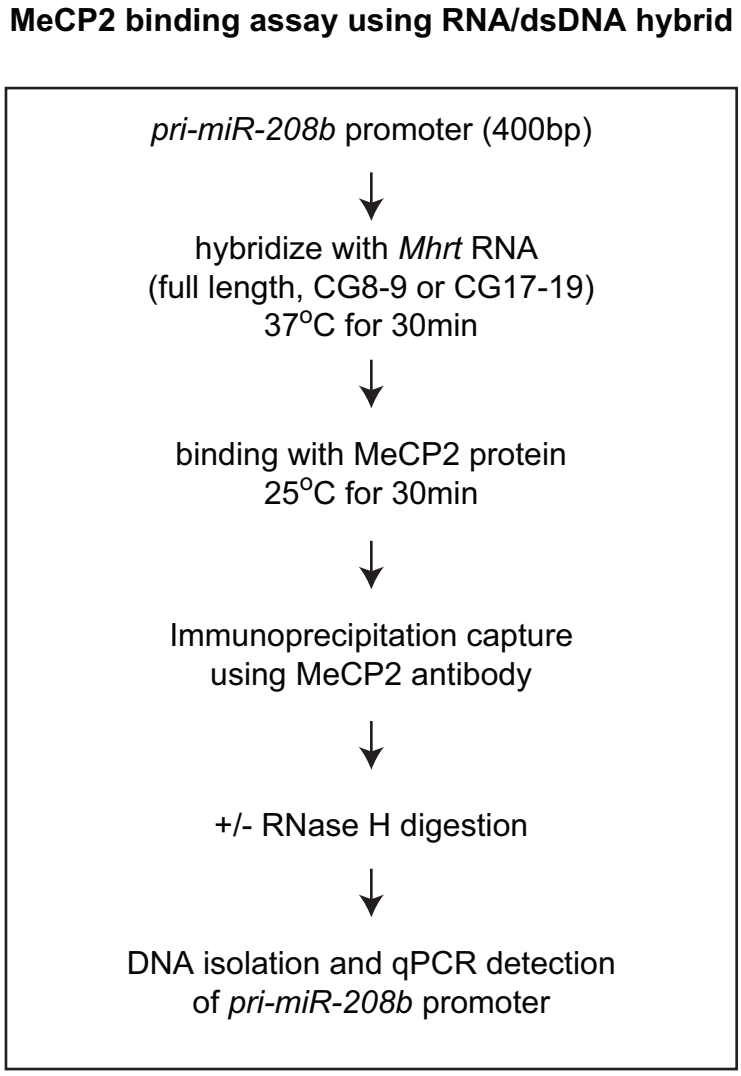

Supplemental Figure S4, related to Figures 3E and 4F. Protocol for the binding assay using dsDNA (*pri-miR-208b* promoter), *Mhrt* RNA (*full length, CG8-9, CG17-19* or *methylated CG17-19*) and rMeCP2 in presence or absence of RNase H.

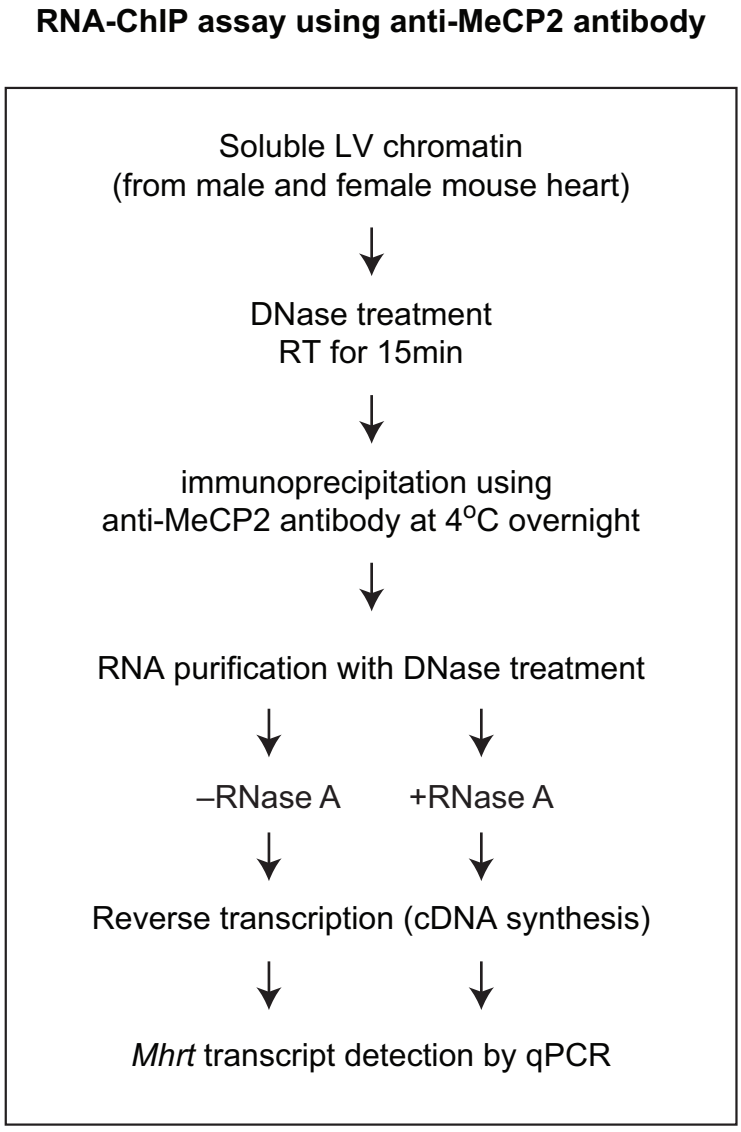

Supplemental Figure S5, related to Figure 4A. Procedure for RNA-ChIP assay using anti-MeCP2 antibody and soluble LV chromatin.

Human *MHRT* sequence

CUGGAGCUGGGACAGGUCAGCAUCCAUCUUCUUCUUCUGGUUGAUGAGGCUGCUGC
UCACCUGGGAAUGCAGCAGCUGCACCCGCUCACUAGUCUCAAUCAGCUCCUGCUCCG
CCAGCUUCCGGGACCGCUCUGUCUGCUCCACCACGGCACGCAACUCCUCCAGCUCAG
CCUGCAGCAGGUUGUUGCGCCGCUCCACGAUGGCGAUGUUCUCCUUCAGGUCGUCG
UUGGCACGGACUGCAUCGUCCAGCUGAAUCUGGGUUACCUUCAACAAGCUCUGGAG
GCUCUUGACUUGCUUCUGGGCCUCGGCGGCCAUGCGGUUGGCGUGGCUGAGCUGGA
UCUCCAUCUCAUUGAGGUCUCCUUCCAUCUUCUUCUUCACCCUCAGGGCCUCGUUGC
GGCUGCGUGUCUCUGCGUCCAGGGAGGUCUGCAGCGAGUCCACCACCCGCAGGUGG
UUGCGCUUGGCCUGUUCCAUCUCCUCGUCCUUCUCUGCCAGCUUCCGCUCGAUCUCU
GCCUUGAUCUGGUUGAACUCCAGCUGGGCCCGGAGGAUCUUGCCCUCCUCCUGCUUU
CGGACCUUCUCCAGCUCAUGGAUAGUCUUUCCGCUGGAACCCAACUGCUCAGUCAAG
UCGGAGAUCUCCUCUGUGUGGGGAACACGGCGUUCUUGAGUUUGAAGAGCUCUGUG
CUGAGGGAGCGAGCCUCCUUCUGCGAGGACUCCAGCUCCGACUGCGACUCCUCAUAC
UUCUGCUUCCACUCGGCCAGGAUCUGCCCGGGGACAAGGCUCACUCUUCAGCCCCCC
AGCCUCAGCCCCAUGUCCAGGGGCUGCAGCAGCAGCAUUGGAGCGCUCUACGUCCAC
CAUCAAGUCCUCGAUCUCAUUCUGUAG

Mouse *Mhrt* sequence

AGCCCUACAGUCUGAUGAACAUUCUAGAGUAUGUGGACACAGAUGGACGCUCUGGC
CACAGCUUGUUGACCUGGGACUCGGCGAUGUCCGCCCUCUCCUCCGCCUCAUCCAGC
UCGUGCUGCACCUUGCGGAACUUGGACAGCCUCCAGCUCAUUCUCCAGCUCCCGGAC
CCGGGCCUCCAGCUUCUGCAGCUGCUUCUUGCCGCCCUUGAGGGCGAUCUGCUCUGC
CUCGUCCAGACGGUGCUGCAAGUCCUUGAUGGUCUGCUCCAUGUUCUUCUUCAUGC
GCUCCAGGUCGUCAUUGGCACGGACAGCAUCAUCCAGCUGGAUUUGAGUGUCCUGA
GGAUCAGAAAAAUGAGUGGCCUCAUUGCGGCUGCGUGUCUCCGCAUCCAGGGAGGU
CUGCAGGGAGUCCACCAUCCGCAGGUGGUUGCGCUUGGCCUGCUCCAUCUCCUCAUC
CUUCUCUGCCAGCUUCCUUUCAAUCUCUGCCUUGAUCUGGUUGAACUCUAGCUGGG
CGCGGAGGAUCUUGCCCUCCUCGUGCUCCAGGGAGGCCUGGAAAGGAUAUAGAUUU
UGCAGGCAUAUAGUCAGAGACCAGGGUGGAAGCAAGGGUGUGUCUAAAAACCAUGG
CACAGAGAGCAUUUGGGGAUGGUAUACAUGACUCAGUAGGAGAUGCAGUGGAAGGA
AAUGAGAAAGAGUGUGCACAAGAGAAAUGAAAGCAAGCUGAAGAGAAGGGGAUGC
AGACUCCCAGGGGGGCGGAGGGAGUCAGCUUUGAAGACAAAGAGGAAAAUGAAAAG
UGUUGCCAAGGAAACAGAGGCAAUGAAGCAGAGAGUAAAGG

Supplemental Figure S6, related to Figure 4B and 4D. CG18 and flanking sequence-is conserved between mouse and human *Mhrt* transcripts.

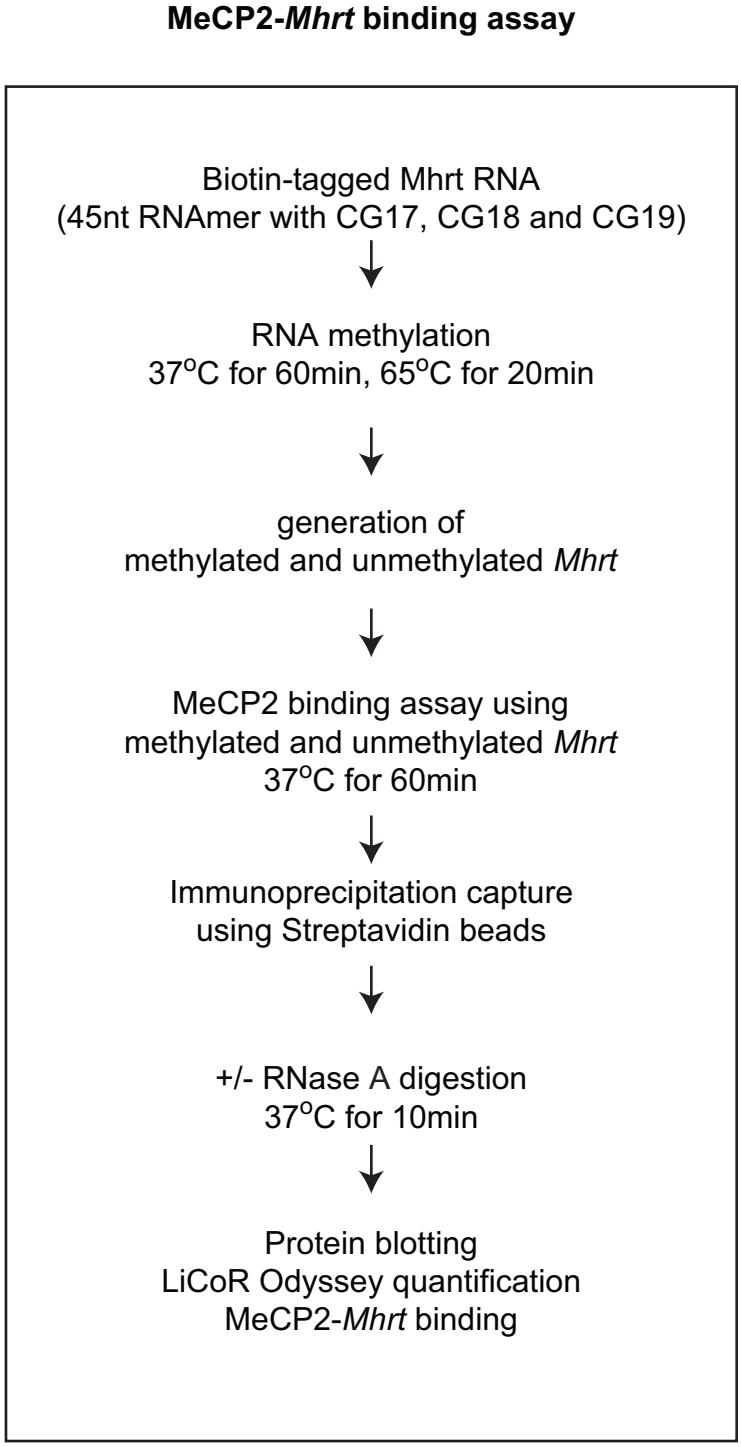

Supplemental Figure S7, related to Figure 4E. Assay designed for assessment of *Mhrt*-MeCP2 binding. Biotin-tagged 45nt long *Mhrt* oligomer was methylated using *Sss1* methyltransferase followed by incubation with recombinant MeCP2. Streptavidin immunoprecipitation of *Mhrt* followed by protein blotting for MeCP2 was quantified by LiCoR Odyssey.

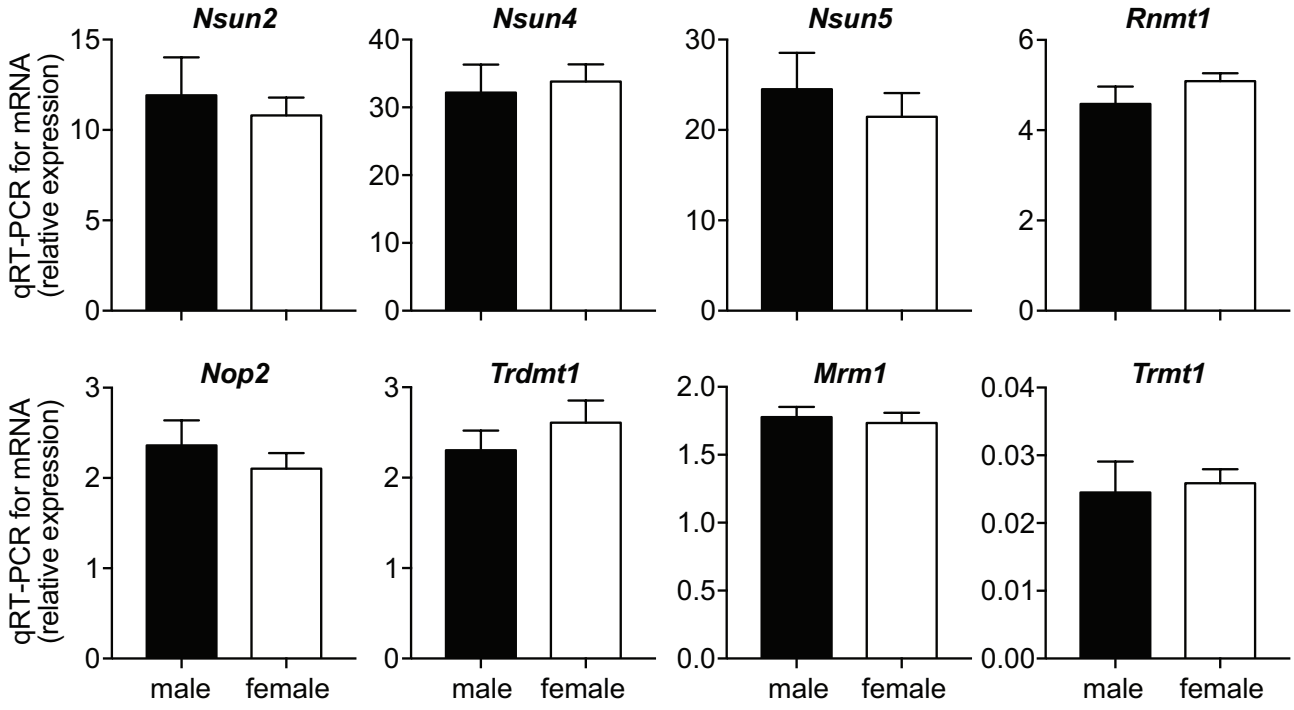

Supplemental Figure S8, related to Figure 4. mRNA expression of known RNA methyltransferases (*Nsun2, Nsun4, Nsun5, Rnmt1*, *Nop2, Trdmt1, Mrm1, Trmt1*) examined by qRT-PCR. n=5 mice per group. Data are represented as mean ±SEM.

Table 1. Transcript Detection Primers

α-MHC Forward	CCACCTGGGCAAGTCTAACAA
α-MHC Reverse	TGTAGTCCACGGTGCCAGC
β-MHC Forward	GATGTTTTTGTGCCCGATGA
β-MHC Reverse	ACCGTCTTGCCATTCTCCG
Mhrt Forward	GCTCTGGCCACAGCTTGTTGACCTG
Mhrt Reverse	CGTGCCAATGACGACCTGGAGCGC
Pri-miR-208b	Taqman Pri-miRNA assay (Mm03308667_pri)
Mecp2 forward	ACCTTGCCTGAAGGTTGGAC
Mecp2 Reverse	AAGCTTTTCCCTGGGGATTGA
Mbd1 Forward	CCTGGTTGCCAAGGCTACATA
Mbd1 Reverse	CAGGTTCAGCTTTTCAGCCA
Mbd2 Forward	CCAAATTCACGAACCACCCG
Mbd2 reverse	CCCAGAAAAGCTGACGTGGT
Mbd3 Forward	TGGGAAAGGGAAGAAGTGCC
Mbd3 Reverse	TCCCGCTGGGGCTATAGTAA
Nsun2 Forward	AGTGGTTTGCAGACTGGCAT
Nsun2 Reverse	CAGGATTCGAAGGCATCGCT
Nsun4 Forward	GACGGGTTGTTGCCGTAATC
Nsun4 Reverse	ACTCGGACTTGGTTCCCTTC
Nsun5 Forward	GTCGTAGAGCGCTTGAGGC
Nsun5 Reverse	GCTTCAGGTTCTGGAAGTTGC
Rnmt Forward	GTGGATGACTGTGTGGTGTC
Rnmt Reverse	GACTCTGGGTCAGAAGCGAC
Nop2 Forward	GCTCTGATCAATCGTGGGGT
Nop2 Reverse	CTCAGGGGTAGCGCCAATAG
Trdmt1 Forward	GGTTGCGAGAGGATGGAAC
Trdmt1 Reverse	TGCAGGGATATGACTTTCTCGC
Mrm1 Forward	AGAGAAACAGCTGTCCGCTTA
Mrm1 Reverse	AAAAACCGGGCAGGTCAGGA
Trmt1 Forward	TTGTCATGTGATTGGCCCGC
Trmt1 Reverse	TCAACCCGCCCGGACAAG

Table 2 ChIP Primers

Pri-miR-208b promoter Forward	TCTGACCCTCTGTGTCCCTGGCT
Pri-miR-208b promoter Reverse	GCCCACCTTGGCCTTGATGA
Intergenic promoter Forward	GAGCCTCAAGTGACCTCCAG
Intergenic promoter Reverse	CTCCAAGGGACCTGATTCAA

Table 3 Bisulphite-Specific Primers

Pri-miR-208b promoter Forward	TTTGATTTTTTGTGTTTTTGGTTAG
Pri-miR-208b promoter Reverse	ACCCACCTTAACCTTAATAATCTACTC
Mhrt Region A Forward	GTAGTGGAAGGAAATGAGAAAGAGTGTG
Mhrt Region A Reverse	CCTCTTTATCTTCAAAACTAACTCCC
Mhrt Region B Forward	GTTTTGATTTGGTTGAATTTTAGTTGGG
Mhrt Region B Reverse	CTATATCCTTTCCAAACCTCCCT
Mhrt Region C Forward	GGATTTGAGTGTTTTGAGGATTAGAAAAATGAGTGG
Mhrt Region C Reverse	CCCAACTAAAATTCAACCAAATCA
Mhrt Region D Forward	GAATTTGGATAGTTTTTAGTTTATT
Mhrt Region D Reverse	CCACTCATTTTTCTAATCCTCAAAACACTC
Mhrt Region E Forward	GAATATTTTAGAGTATGTGGATATAGATGG
Mhrt Region E Reverse	AACTAAAAAATAAACTAAAAACTATCC
mAsp Forward	TGTTAGTATAGTGGTGAGTAT
mAsp Reverse	CTCCCCATCAAAAAATTA